



# Additive Manufacturing of Carbon Fiber-reinforced Composites: A Review

Yong Hu<sup>1,2</sup> · Yudong Lin<sup>1,2</sup> · Lei Yang<sup>1,2,3</sup> · Siqi Wu<sup>3</sup> · DianYu Tang<sup>1,2</sup> · Chunze Yan<sup>3</sup> · Yusheng Shi<sup>3</sup>

Received: 2 May 2023 / Accepted: 4 November 2023 / Published online: 8 December 2023  
© The Author(s), under exclusive licence to Springer Nature B.V. 2023

## Abstract

Carbon fiber-reinforced composites (CFRCs) have been widely used in automotive, aerospace, sports equipment, and other industrial fields, due to the higher strength-to-weight ratio and modulus compared with metals and alloys. Innovations in additive-manufactured CFRCs have opened up new avenues for designing and manufacturing high-performance, low-cost complex composite structures. According to the structure and substrate type of carbon fiber, this paper firstly reviews the existing feasible technologies as well as their key elements and focuses on the research of additive manufactured CFRCs by fused deposition molding (FDM) and selective laser sintering (SLS). Furthermore, the typical applications and envisions of additive manufactured CFRCs were elaborated. Moreover, the existing challenges and problems are summarized from the aspects of materials, equipment, and software. In the future, more interdisciplinary research is needed on advanced materials, multiple processes, advanced equipment, and structural design, and there will be a broader research space for robot-assisted additive manufacturing and green manufacturing methods.

**Keywords** Additive manufacturing · Carbon fiber-reinforced composites (CFRCs) · 3D printing · Forming quality · Robot-assisted additive manufacturing · Green manufacturing

## 1 Introduction

Carbon fiber-reinforced composites (CFRCs) have the characteristics of lightweight, high strength, high-temperature resistance, and corrosion resistance, and have been used in various fields of military and civilian industries. The preparation of carbon fiber reinforced

---

✉ Lei Yang  
lei.yang@whut.edu.cn

✉ Chunze Yan  
c\_yan@hust.edu.cn

<sup>1</sup> School of Transportation and Logistics Engineering, Wuhan University of Technology, Wuhan, China

<sup>2</sup> Hubei Longzhong Laboratory, Xiangyang, China

<sup>3</sup> State Key Laboratory of Materials Processing and Die & Mould Technology, School of Materials Science and Engineering, Huazhong University of Science and Technology, Wuhan, China

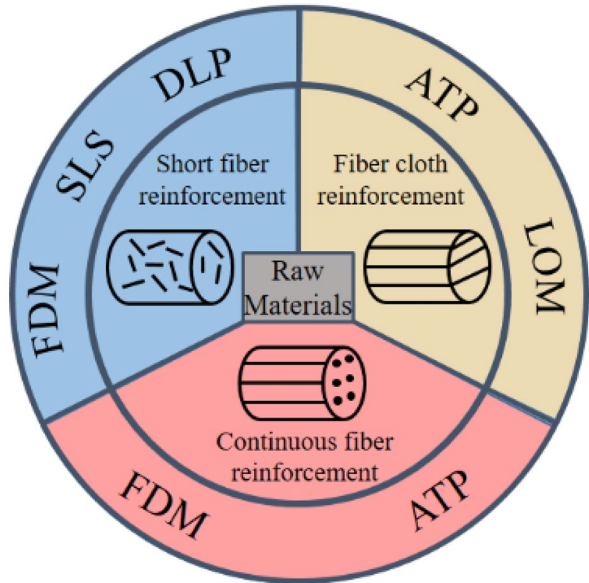
composite parts by traditional processes usually requires the preparation of carbon fiber prepregs, pre-laying the prepregs on the mold, hot-press forming in the autoclave, and finally machining and assembly. When using traditional processes to prepare carbon fiber reinforced composite parts, it faces problems such as large initial investment, high operating cost, long manufacturing cycle, and low material utilization rate. More importantly, it is difficult or even impossible to form complex parts at once [1, 2].

Additive manufacturing (AM) takes layered manufacturing as the molding principle and integrates CNC, material science, computer-aided design, and other advanced technologies, which makes it feasible to fabricate precise structures [3, 4]. The 3D models are sliced to obtain two-dimensional profile information for each section. Under the control of the control system, the print head of the 3D printer prints layer by layer according to the input profile information, and finally forms a three-dimensional workpiece. Stereo lithography apparatus (SLA), fused deposition molding (FDM), selective laser sintering (SLS), selective laser melting (SLM), laminated object manufacturing (LOM), and automated tape placement (ATP) are the typical AM technologies [5–7].

With the development of AM technologies, additive manufacturing of CFRCs is gradually becoming feasible. The use of carbon fiber to strengthen the matrix can be divided into three types: short fiber reinforcement, continuous fiber reinforcement, and fiber cloth reinforcement [8, 9]. The available additive manufacturing processes vary for different reinforcement types of raw materials. FDM, SLS, and DPL can be used for short carbon fiber-reinforced raw materials, ATP and LOM for fiber cloth-reinforced raw materials, and FDM and ATP for continuous fiber-reinforced raw materials.

The research on additive-manufactured CFRCs is increasing year by year and gaining more attention. A review of research on additive manufacturing of fiber-reinforced thermoplastic composites was published by Pervaiz et al. [10] in 2021. The mechanical properties of carbon fiber-reinforced composite fabrications prepared by the FDM process were reviewed and machine learning was proposed as a new research direction in this field. The review by Adil et al. [11] focuses on manufacturing accuracy and mechanical properties. Tian et al. [12] provides an overview of the latest technologies based on the relevance of materials, structures, processes, properties, and functionality of CFRCs. These reviews have provided a comprehensive summary of the process characteristics, mechanical properties, market applications, and an outlook on future research trends for additively manufactured CFRCs. However, the prepreg is also an important factor affecting the Fig. 1 additive manufacturing of CFRC parts, and the prepreg preparation process is rarely mentioned in these reviews. In addition, the process window is one of the first issues to be explored in the study of any additive manufacturing process, and it is necessary to summarize the process parameters obtained by previous generations through experiments and other means. Therefore, in this paper, a more comprehensive review of additive manufactured CFRCs, including the prepreg feedstocks, AM processes, and equipment, are reviewed. We focus on the two additive processes most commonly used in fiber-reinforced composites, FDM and SLS. The additive manufacturing of CFRCs is explored from a multi-process perspective as a way to broaden the thinking on additive manufacturing of CFRCs. Also, the existing applications of CFRCs are described and a future outlook on AM of CFRCs is given. It is hoped that through this literature review, readers will be able to get a quick grasp of what is being researched in the field, find their way to the research, and be able to solve some of the problems encountered in the research.

**Fig. 1** Three different carbon fiber-reinforcement types and their applicable AM processes



## 2 CFRC Raw Material Preparation and Modification Technology

Obtaining excellent CFRC feedstock is the first step in additive manufacturing of CFRC parts, so it is necessary to review prepreg preparation methods and carbon fiber modification methods.

### 2.1 Preparation of Short Carbon Fiber-reinforced Composite Filaments

The screw extruder is the main equipment to realize the preparation of short carbon fiber-reinforced composite (SCFRC) filaments, as shown in Fig. 2. The process can be divided into three steps. First, the short carbon fiber and the resin are fed into the high-speed rotating mixer. Then, the mixture is fed into a high-temperature extruder, where the resin is heated and melted onto the surface of the carbon fiber and extruded into filaments. Finally, the filament composite material is sent to the cooling bin for cooling [13]. To obtain a more homogeneous composite filament of each component, the initially formed composite filaments can be shredded, fed again into a high-temperature extruder for extrusion, and finally extruded to form new filaments [14].

### 2.2 Preparation of Continuous Carbon Fiber-reinforced Composite Filaments

The preparation of continuous carbon fiber-reinforced composite (CCFRC) filaments usually uses the method of prepreg impregnation. The carbon fiber is passed through the prepreg solution at a uniform speed so that the matrix enters the void of the carbon fiber to form CCFRC filaments [15]. As shown in Fig. 3, the winding wheel 5 is the active wheel and is responsible for pulling the carbon fiber out of winding wheel 1. The

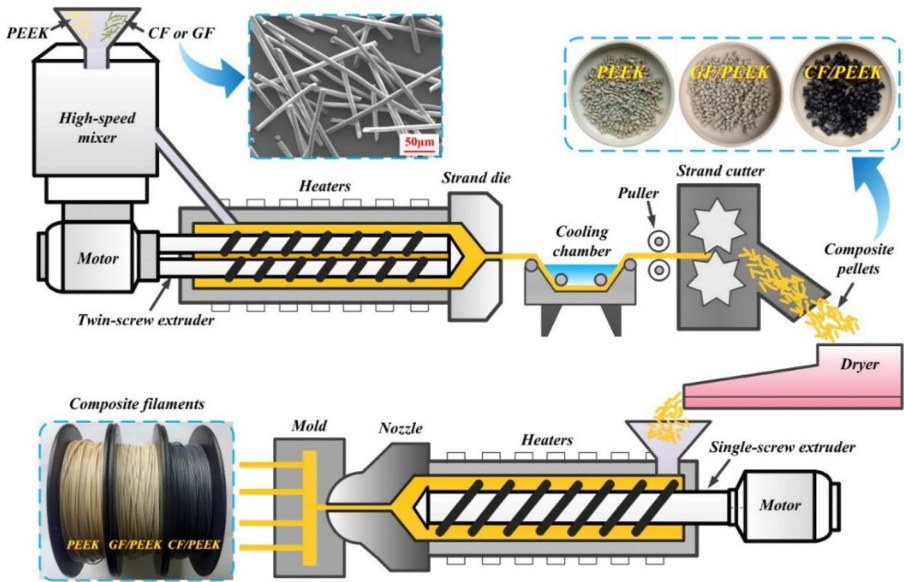


Fig. 2 Preparation process of SCFRC filaments [14]

pulled-out carbon fiber bundle is heated and softened in heating bin 2 and then goes to the impregnation tank 3 for impregnation. The carbon fiber bundles spread out as they pass around impregnation roller 4 so that the resin can evenly encase each carbon fiber. Finally, the impregnated carbon fiber prepreg is incorporated into winding wheel 5.

This method is a general way for preparing CCFRC filaments, which can be applied to prepare CCFRC filaments of a variety of substrates, including PLA, ABS, and Nylon. The researchers have made many improvements in filaments feeding, and collecting to strengthen the binding between the carbon fiber and the matrix for better mechanical properties. Among them, the impregnation of carbon fibers is the key step to the quality of CCFRC filaments. A better impregnation can lead to a more even dispersion of carbon fibers in CCFRC filaments, thus improving the quality of carbon fiber additive manufacturing

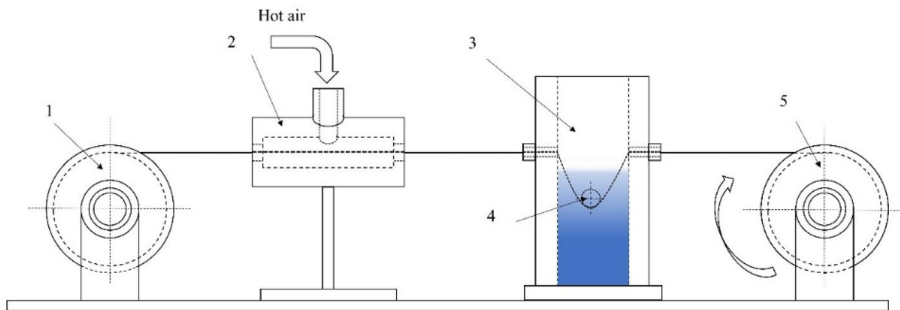


Fig. 3 Preparation process of CFRC filaments [15]: 1. Unwinding wheel, 2. Heating bin, 3. Impregnation tank, 4. Impregnation roller, 5. Winding wheel

parts from the raw material side. The impregnation quality of the matrix can be improved by multiple impregnations of the carbon fiber, fiber spreading, or the use of an external device. Three different impregnation methods are shown separately in Fig. 4. Figure 4a shows the method of roller group spreading. The wrap angle of continuous carbon fiber is controlled by changing the relative placement of the rollers to achieve a better spreading effect. A take-up port is provided at the end of the machine to control the diameter of the carbon fiber bundles, thus preparing prepregs with different carbon fiber contents. Figure 4a shows an impregnating roller with a unique design and a prepreg take-up unit, using which prepregs with a uniform degree of fiber dispersion are successfully prepared [16]. Figure 4b shows an ultrasonic impregnation method in which an ultrasonic impregnation device is placed in the impregnation tank and the resin in the molten state is assisted by ultrasonic vibration to adhere to the surface of the continuous fiber yarn for better wrapping. The device was not set up with a separate take-up port, so the diameter of the prepreg could not be controlled. In the case of the device shown in Fig. 4c, a prepreg take-up device is set up, and the PLA in the molten state is placed at a higher pressure by the single-screw extruder. Under this pressure, the resin-coated carbon fiber filaments are pulled out at the nozzle confined to a certain diameter range. The heating device keeps the carbon fibers dry, ensuring that the carbon fibers are easily impregnated by the molten resin. After finishing the maceration, the composite filaments are sent to cooling water to solidify and finally wrapped into rolls for later use.

All the above three methods are assisted by external devices to facilitate the bonding of the resin to the continuous carbon fiber filaments, utilizing only the original physical properties of the resin and the carbon fiber. To make the resin firmly and uniformly distributed on the surface of continuous carbon fiber filaments, adding grooves on the surface of continuous carbon fiber to increase the roughness, changing the chemical bonding on the surface of continuous carbon fiber, and adding a layer of substance as an intermediate to absorb the resin and carbon fiber together maybe some new ways to prepare continuous carbon fiber prepreg. The properties, advantages, and disadvantages of some resin materials commonly used for FDM are shown in Table 1 [20].

### 2.3 Interfacial Modification

CFRC filaments are three-phase structures that include carbon fibers, resins, and interfaces. After high-temperature carbonization, carbon fiber is difficult to infiltrate by the resin, due to the inert surface. In recent years, it has been widely recognized that the micro toughness effects of nanomaterial surfaces can effectively change the interfacial properties of CFRCs. Graphene and carbon nanotubes are the two most commonly used nanomaterials for surface modification of carbon fibers [21, 22]. Currently, the use of nanomaterials to change the interface between carbon fiber and resin is mainly through two ways: adding different raw materials and discovering new wrapping methods. Figure 5a and b show the effect of electrophoretic deposition and graphene/carbon nanotubes to enhance the interface, respectively [23, 24]. It can be seen that both angles can increase the surface roughness of carbon fibers, promote the bonding of carbon fibers with resin, and ultimately improve the interlaminar shear strength of carbon fiber-reinforced composites. For the former, the surface of the carbon fiber can also be treated by the addition of an active agent or by using an ultrasonic device to assist the deposition. [25, 26]. For the latter, a combination of various nanomaterials such as carbon nanotubes, graphene, copper nanomaterials, and silica nanoparticles can be utilized to achieve the effect of modifying the interface [27, 28].

**Table 1** Key properties and applications of additive manufacturing filaments: material, extruder temperature ( $T_e$ ), bed temperature ( $T_b$ ), glass transition temperature ( $T_g$ ), advantages, disadvantages, and applications

Material	$T_e$ (°C)	$T_b$ (°C)	$T_g$ (°C)	Advantages	Disadvantages	Resin types
PLA	160 ~ 230	20 ~ 60	60 ~ 65	Biodegradable, non-toxic, low cost	Tough, strong	Thermoplasticity
ABS	215 ~ 250	80 ~ 110	104 ~ 109	Heat-resistant, strong, durable	Needs high temperature and hot bed, toxic, Affected by humidity	Thermoplasticity
PA6	240 ~ 260	70 ~ 100	55 ~ 65	Tensile, compressive, and abrasion resistant	Easy to absorb water, poor lightfastness	Thermoplasticity
TPU	210 ~ 230	30 ~ 60	-35	Low-temperature resistance	Not heat resistant	Thermoplasticity
PEEK	340 ~ 440	110 ~ 150	143	Excellent lubricity and corrosion resistance	Needs high temperature and hotbed	Thermoplasticity
Epoxy resin	100 ~ 150	100 ~ 150	45	Rigidity, hardness, high-temperature resistance	Other additives required	Thermoset

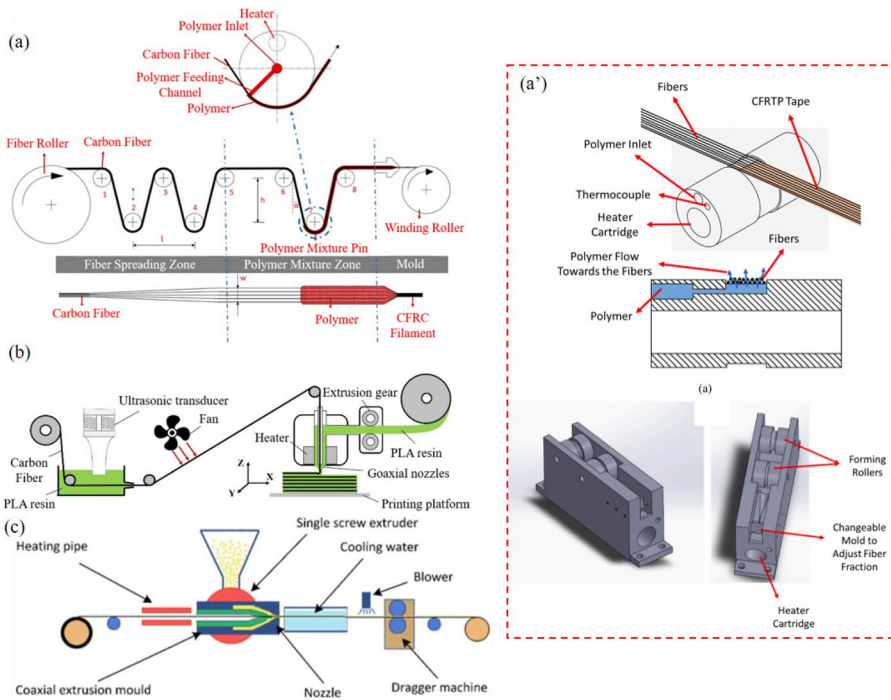


**Fig. 4** Continuous fiber prepreg preparation process: **a** Filament impregnation line of CCFRC filaments [16, 17]; **b** Ultrasonic assisted AM devices [18]; **c** Single screw extrusion resin prepreg filaments making principle [19]

## 2.4 Surface Modification of Carbon Fiber

The addition of carbon fibers to the powder feedstock used in the SLS process tends to cause agglomeration of the carbon fibers. This problem can be improved by surface modification of carbon fibers. Carbon fiber surface modification methods include chemical, electrochemical and plasma treatments. The chemical method is easy to use in the laboratory and does not degrade fiber properties, so it is the preferred method for surface modification of carbon fibers [29]. Modification of the surface of carbon fiber can increase the surface area and surface activity of the fiber, thereby affecting the roughness of the surface of the carbon fiber and the dispersion in the coated sand. Using hydroxyethyl fiber (HEC) as a dispersant for short carbon fibers can effectively improve the dispersibility of carbon fibers. The addition of concentrated nitric acid and coupling agent modification can increase the groove on the surface of the carbon fiber, and its roughness is greatly increased, making the interfacial performance of the compound more excellent [30]. As shown in Fig. 6a to c, they show the carbon fiber surfaces treated in one of three ways: untreated, treated with concentrated nitric acid, and treated with a mixture of concentrated nitric acid and coupling agent KH550. Carbon fibers treated with a mixture of concentrated nitric acid and coupling agent KH550 have the highest roughness [31]. As shown in Fig. 6d to f, Jing et al. [32] treated carbon fibers with concentrated nitric acid and prepared parts from the treated carbon fibers. It was found that the functional groups of carbon fibers treated with concentrated nitric

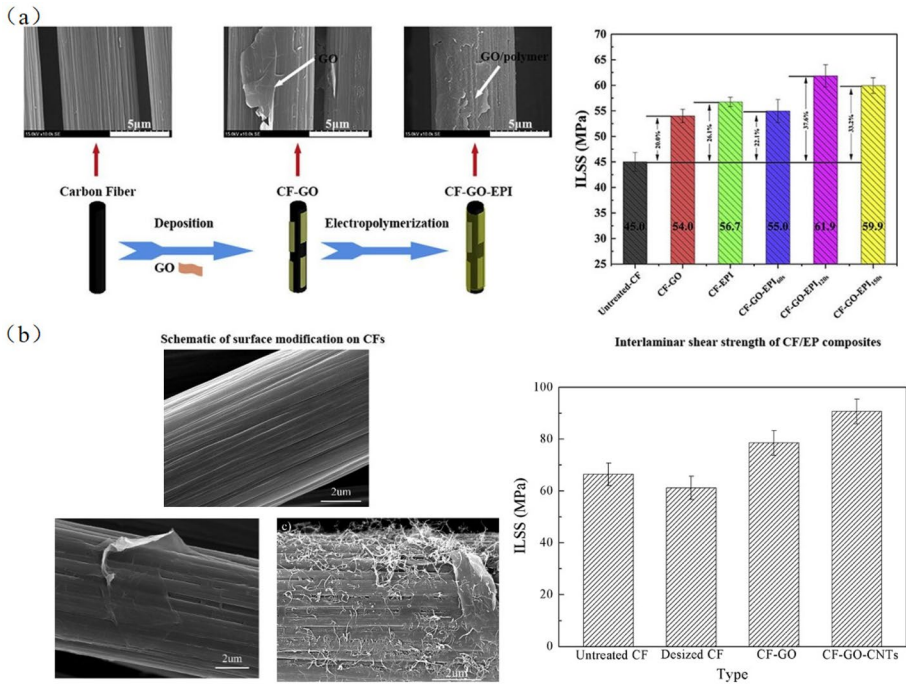


**Fig. 5** Carbon fiber surface modification methods: **a** Electrophoretic deposition [23]; **b** Multi-nanomaterial hybrid modification method [24]

acid were thermally decomposed into gases during the sintering process, and the porosity of the parts increased accordingly. The carbon fiber mixture treated with concentrated nitric acid is further treated at 400 °C in a nitrogen environment, which can retain some of the modification effects while reducing the porosity of the composite.

### 3 AM Processes and Equipment

#### 3.1 Fused Deposition Molding

FDM is computer-controlled and uses a layer-by-layer manufacturing method to produce parts made from thermoplastic resins. This AM technology selectively heats and melts various thermoplastic filaments and prints them in a predetermined path on a molding table. The manufacturing process includes 3D model design, slicing, data transferring to the printer, and layer-by-layer printing until the model is completed [33]. It is the most widely used AM technology because of its ease of use, low cost, smooth operation, and safety. Manufacturing CFRC parts by FDM is similar to manufacturing thermoplastic resin parts by FDM, in which carbon fiber prepreg is fed into a nozzle to be heated and melted, and then extruded from the nozzle to be deposited on a platform for solidification. Currently, FDM technology for CFRC can be divided into single input–single output manufacturing method, multiple input–single output manufacturing method, and multiple input–multiple output manufacturing method [34–36].



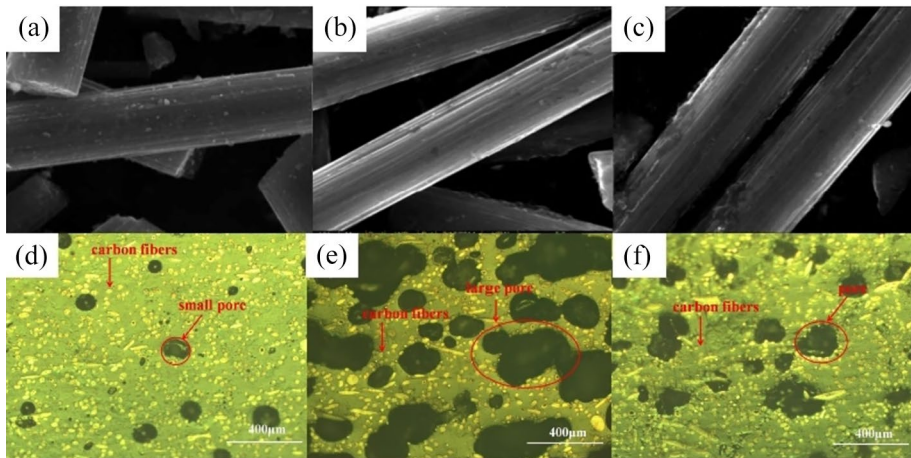


**Fig. 6** Short carbon fiber surface morphology: **a** Unmodified **b** Concentrated nitric acid modification **c** Coupling agent and concentrated nitric acid modified at the same time [31]; Cross-sectional morphology of carbon fiber-reinforced nylon 12 composites: **d** Untreated **e** Concentrated nitric acid modified treatment **f** Concentrated nitric acid modified heat treatment [32]

### 3.1.1 Single Input-Single Output Manufacturing Method

The single input-single output manufacturing method is most commonly used to print thermoplastic resin. The preparation of prepreg provides the conditions for additive manufacturing of CCFRC parts. As shown in Fig. 7, the single input-single output FDM additive manufacturing method involves heating and melting the prepreg directly into the nozzle, and then extruding it from the nozzle. This method is convenient and fast and enables the printing of both CCFRC filaments and SCFRC filaments. It should be noted that CCFRC filaments are easily scraped when passing through the nozzle, therefore, FDM nozzles used for printing CCFRCs are often treated with special treatments, such as adding chamfers and enlarging the nozzle aperture [37], And the nozzle diameter is larger than the diameter of CCFRCs is one of the reasons for the loss of accuracy in manufacturing CCFRC parts [38].

### 3.1.2 Multiple Input-Single Output Manufacturing Method

The multiple input-single output manufacturing method refers to that multiple feed ports are set at the nozzle, so that different raw materials enter the same heating bin at the same time for feeding and mixing [39–41]. It includes two manufacturing methods: in-situ impregnation and co-extrusion of filament bundles. As shown in Fig. 8, in-situ impregnation means that dry continuous fibers and filamentous resin are fed into the heated bin at the same time, and the fibers and resin are mixed in the heated bin. Filament bundle co-extrusion is based on in-situ impregnation by replacing dry carbon fibers with carbon fiber prepreg, enabling the mixing and printing of multiple substrates. Multiple input-single output manufacturing method can be used to print on higher viscosity substrates, such as TPU, PETG, etc. [42, 43]. However, high-viscosity resin tends to make carbon fiber extrusion difficult, which can lead to nozzle clogging. To solve this problem, Ye et al. [44] added

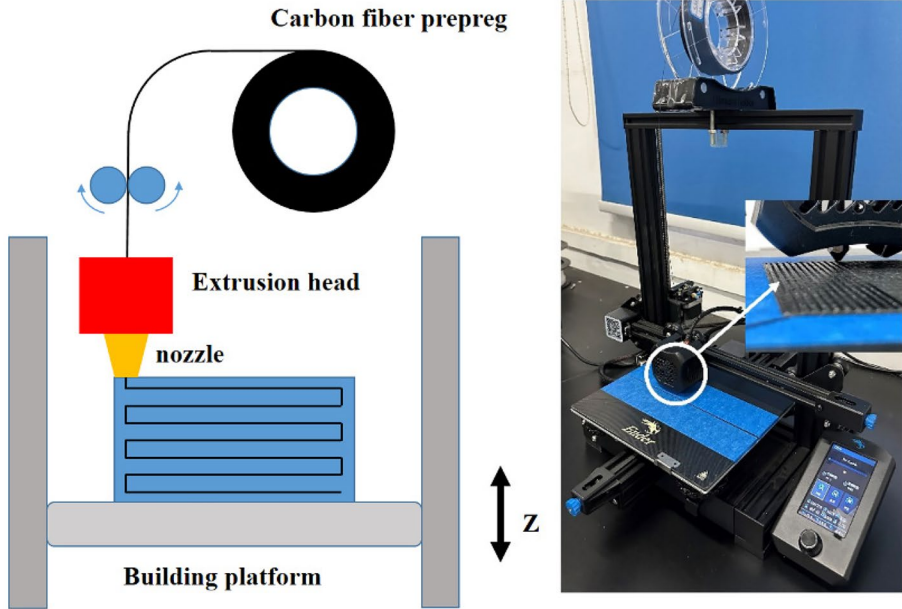


**Fig. 7** Single input-single output manufacturing method

a concentric tube at the front 3 mm of the nozzle to shorten the contact time between TPI and carbon fiber, which in turn allowed TPI and carbon fiber to extrude smoothly into the nozzle and be printed.

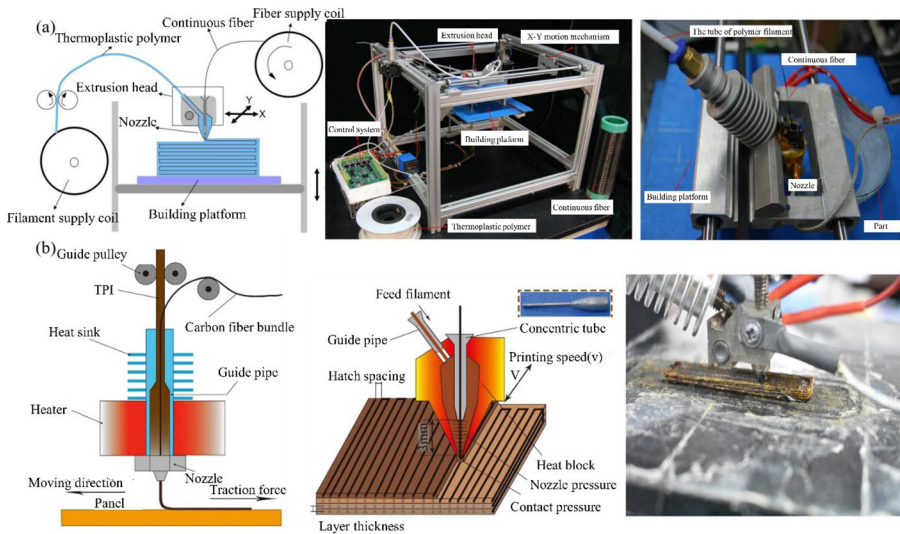


**Fig. 8** In-situ impregnation equipment and principles: **a** Multiple input-single output manufacturing method [45]; **b** Printers with concentric tubes [44]

### 3.1.3 Multiple Input-Multiple Output Manufacturing Method

Multiple input-multiple output manufacturing method utilizes multiple tubes to introduce the substrate and carbon fiber separately, and then multiple nozzles are used to print the carbon fiber and substrate separately. In this process, the substrate and carbon fiber do not touch each other inside the print head. As shown in Fig. 9, this printing method prints the carbon fiber and substrate separately so that the carbon fiber and substrate are combined in a layer-by-layer bond. This method allows the extrusion rate of carbon fibers and matrix to be controlled separately, achieving flexible control of the carbon fiber content [46]. At the same time, since the carbon fiber and the substrate are not in contact with the print head, the carbon fiber is prevented from clogging the nozzle due to the over-sticky substrate, and a more stable printing rate and material extrusion rate is obtained.

### 3.1.4 External Curing Device to Assist Manufacturing

For carbon fiber-reinforced thermoset resin composites, general FDM equipment can often only perform the thermoset composite filaments because the nozzle temperature has not reached the curing temperature of the thermoset resin. As shown in Fig. 10a, the thermoset resin printed by FDM is still in a molten state and not fully solidified. After the part is printed, the part needs to be post-processed, such as autoclave curing or light curing. The autoclave curing method involves burying the molded sample in sodium chloride powder, applying pressure with an external vacuum pump to promote the filling of internal pores and eliminate trapped air, and finally curing the entire device in an oven [47]. The method is cumbersome and takes too long from the start of printing to full molding. In recent years, the addition of a curing device at the print head is a new modification to FDM devices. This technology is called continuous carbon fiber-reinforced thermoset resin in-situ solidification technology, which enables continuous printing and curing of carbon fiber-reinforced thermoset composites into shape. As shown in Fig. 10b, a laser curer is mounted on the print head to cure the resin, and the laser beam is shot slightly offset in the opposite direction of the print path, so that the thermoset resin does not cure as soon as it exits the nozzle, avoiding blocked resin flow [10, 48, 49].

## 3.2 Selective Laser Sintering

SLS technology uses laser-sintered powders to produce parts based on computer-aided design (CAD) models in a continuous layer-by-layer fashion [50]. As shown in Fig. 11,

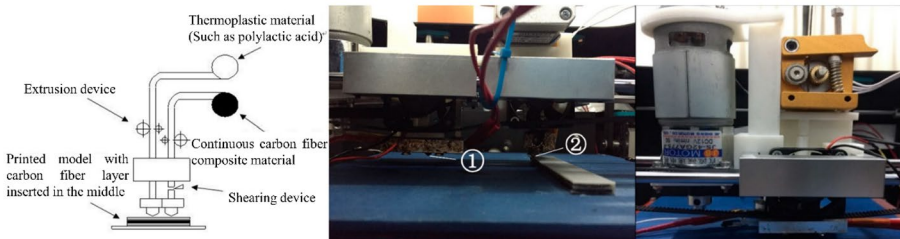


**Fig. 9** Multiple-input and multiple-output manufacturing method [35]

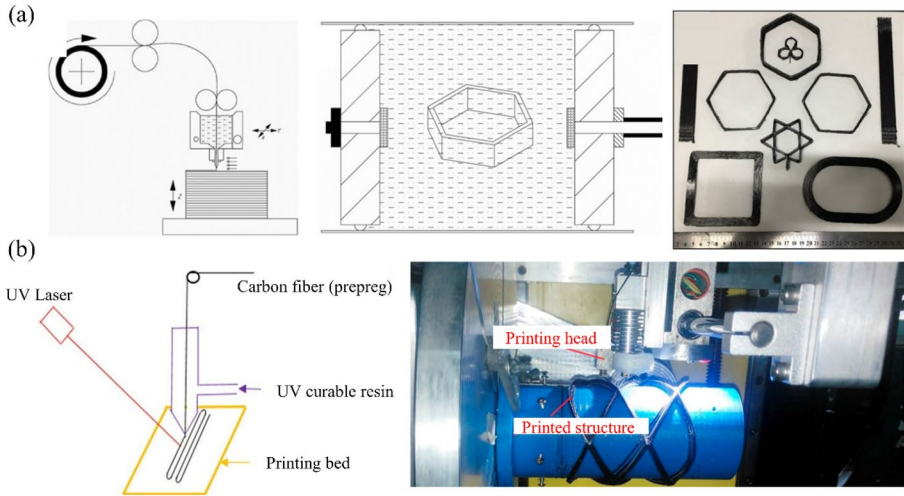


**Fig. 10** Curing method for continuous carbon fiber reinforced thermosetting resin: **a** Additive manufacturing and autoclave curing of carbon fiber-reinforced thermoset composites [47]; **b** Laser-assisted additive manufacturing of carbon fiber-reinforced thermoset resin composites [48, 49]

the SLS system typically consists of a laser, an automatic powder layering device, a computer system for process control, and some auxiliary mechanisms [51].

Polymer powders are the most widely used materials in SLS technology, with PEEK, polyamide and polystyrene commonly used. [53]. In recent years, the application of short fibers in SLS has also received attention from researchers, such as carbon fibers, glass fibers, jute fibers and graphene nanosheets. The incorporation of these short fibers can significantly improve the mechanical properties of the parts. The addition of these staple fibers can significantly improve the mechanical properties of the parts [54–57]. Due to process limitations, continuous carbon fibers are difficult to use as a feedstock for SLS. Adding short carbon fibers or carbon fiber powders to the matrix is a common method for preparing polymer parts from SLS [58, 59]. Carbon

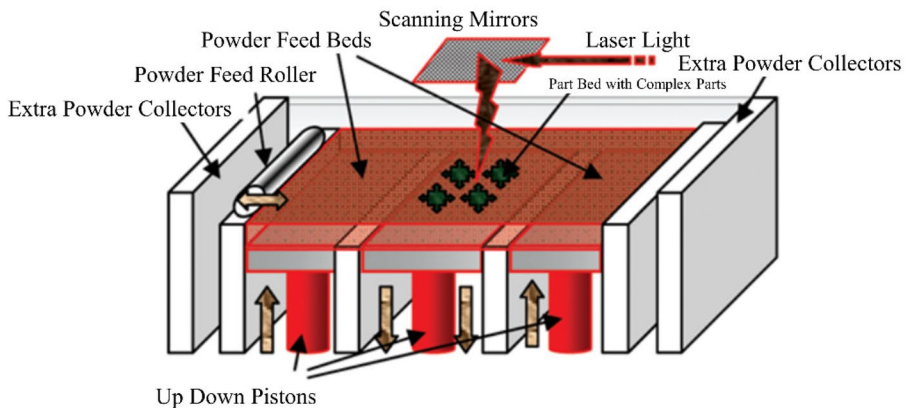


**Fig. 11** SLS printed schematic [52]

fiber parts prepared by SLS have higher surface accuracy, but are difficult to match the mechanical properties of continuous carbon fiber parts prepared by other additive manufacturing methods.

### 3.3 Newly Emerged Process Technologies

#### 3.3.1 Light-curing Additive Manufacturing (Lc-AM)

At present, the AM process of CFRCs focuses on FDM and SLS, while FDM has a natural advantages in the CCFRCs additive manufacturing due to its process characteristics. However, among many printing technologies, the printing accuracy of FDM is not ideal, and it is easy to generate more pores during the printing process. To obtain a finer surface quality, sanding the molded sample is one of the common means, but this method may affect the mechanical properties of the sample. Exploring a new way of printing CFRCs will be a new research direction. Light curing molding technology is one of the earliest AM technologies with high surface accuracy of printed samples. However, the photosensitive resin is sensitive to light, the crosslinking process will cause the part to become brittle, and the molded sample will be warped and deformed over time, requiring a lot of post-processing to retain the geometry of the part [60]. Reinforcement of photosensitive resins using carbon fibers is a viable method to reduce brittleness. As shown in Fig. 12, As if [61] proposed a

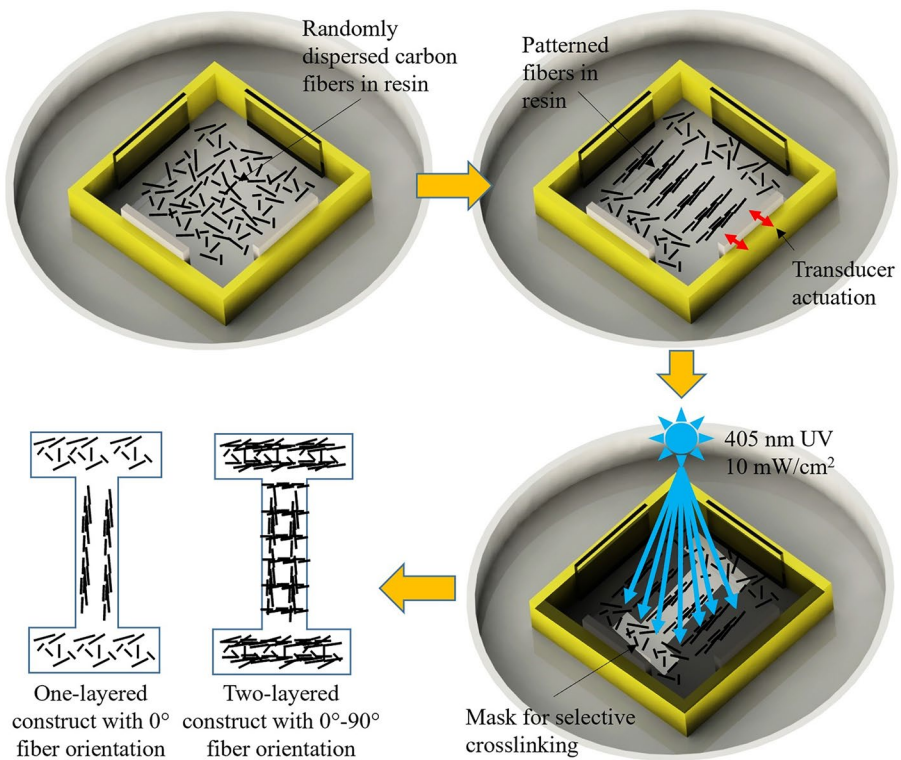


**Fig.12** Schematic diagram of the fiber arrangement of ultrasonically driven and cured resin in the shape of a dog bone specimen using a UV absorption light source [61]

method to organize short carbon fibers in a light-curing resin using the acoustic radiation force of ultrasonic standing waves, thereby realizing the arrangement of short carbon fibers and controlling fiber orientation. This approach is expected to be extended to DLP and SLA processes to create functional mechanical anisotropic composite parts.

### 3.3.2 Robot-assisted Additive Manufacturing (Ra-AM)

In addition to traditional additive manufacturing methods, robots are expected to become a new additive manufacturing method for CFRCs parts. The six-axis robot robotic arm has a high degree of freedom. It can be suitable for any trajectory or angle of work. Flexible and versatile hand-gripped components make Ra-AM a viable continuous carbon fiber additive manufacturing method. Traditional additive manufacturing systems are mostly box-type equipment, and the improvement of the equipment is more complicated, while the robot is an open equipment, with higher operability and a more convenient way to improve the equipment. At present, AREVO has started to use robots for 3D printing. As shown in Fig. 13, the device is a Ra-AM system including a filament feed mechanism, a laser, a press roller, a positioning table, and a filaments shearing device. The basic principle is similar to direct energy deposition (DED). The prepregs are fed to the press roller by feeding mechanism. The laser illuminates the surface of the prepregs to makes the resin melt. After the printing is completed, the prepregs are cut off by the filaments shearing device. This device solves the problem of clogging the nozzles of conventional extrusion printers, allowing CFRC prepregs to be printed smoothly onto the platform. Besides, with the help of the pressing wheel roller, the interlaminar shear strength is expected to be improved. In the future, with the update of robot equipment and the development of technology, there will be a broader research space for Ra-AM of carbon fiber composites.

### 3.3.3 Green Manufacturing (GM)

With the increasing use of carbon fiber-reinforced composites and the increasing amount of waste generated, the recycling of carbon fibers has become a new research direction. Poor recyclability of materials due to the heterogeneity of intrinsic matrix and reinforcing materials, especially for thermoset composites [63]. Jeong et al. [64] use water vapor from 600 °C to 800 °C as an oxidant to remove resin from composites, resulting in a 100% recovery rate of carbon fibers, but its tensile strength is only 66% of the original. As shown in Fig. 14a,

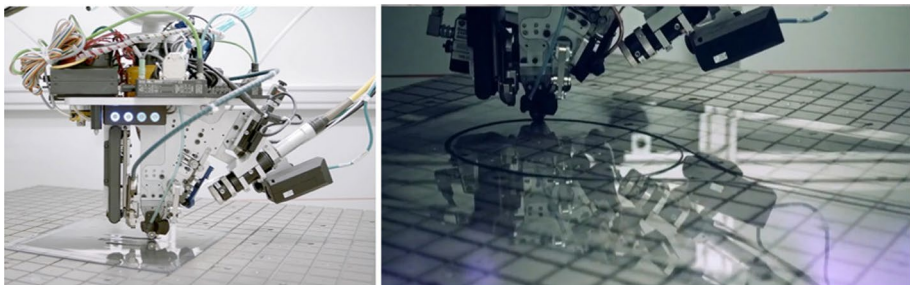
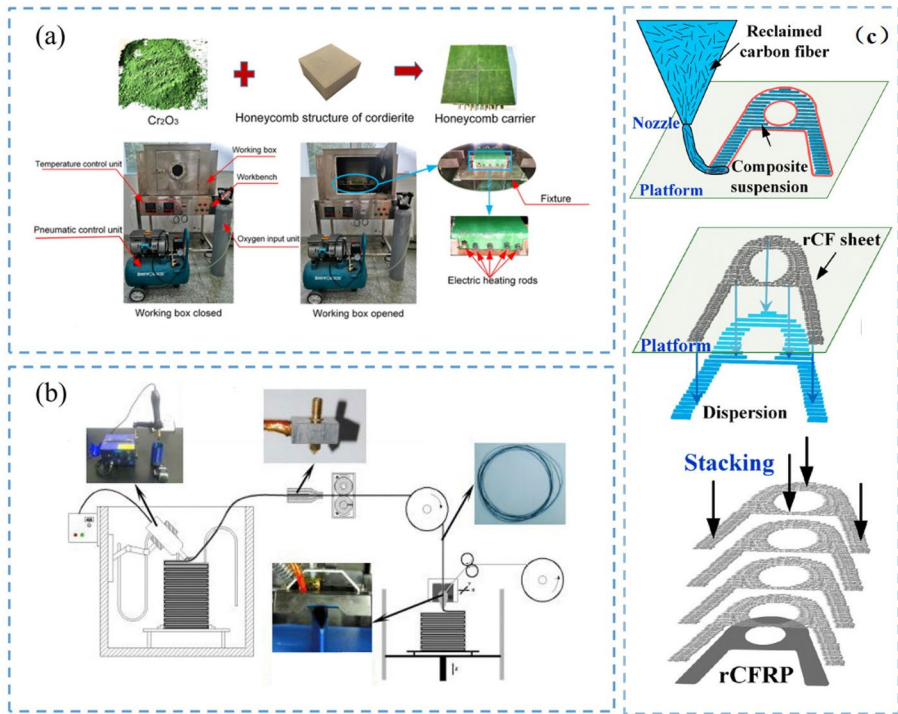


Fig. 13 Ra-AM developed by AREVO [62]



**Fig. 14** Green additive manufacturing process: **a** Scheme of recycling and remanufacturing of additively manufactured continuous carbon fiber-reinforced thermoplastic composites [65]; **b** Equipment diagram for carbon fiber recycling [66]; **c** Layered bonded CFRC re-manufacturing method [67]

Tian et al. [65] proposed a new recycling process for carbon fiber composites. This process can be thought of as an inverse of FDM, where the carbon fiber is gently and continuously pulled out as the hot air gun moves. The recovered thermoplastic-impregnated carbon filaments can be rolled up or sent directly back to the additive manufacturing process for remanufacturing. This method maintains a 100% carbon fiber recovery rate and a 73% PLA recovery rate, while also maintaining the high mechanical properties of carbon fiber. Chen et al. [66] adds  $\text{TiO}_2$  and  $\text{Cr}_2\text{O}_3$  to the recovered carbon fiber, thereby separating the matrix on the surface of the carbon fiber and completing the recovery of the carbon fiber, and the process is shown in Fig. 14b. This recovery method can obtain soft, fluffy, silky carbon fibers, and the decomposition rate of the epoxy matrix has reached 100%. In the future, sustainable development should be achieved by using recycled or green raw materials and innovative additive manufacturing processes. Huang et al. [67] recycled and reused the discarded carbon fiber composites and prepared the CFRC fabricated parts by first printing layer by layer and then bonding them in layers, the process is shown in Fig. 14c.

In addition, the heating of the resin tends to produce a certain amount of emissions, which inevitably generates a certain amount of pollution, whether in the process of filament making or printing. Measuring process emissions can help people mitigate environmental pollution, which is an important part of green manufacturing. Literature [68] gives us some new insights.

## 4 Mechanical Properties of Additively Manufactured CFRC Parts

### 4.1 Key Factors of FDM Forming Quality

To obtain CFRC parts with better mechanical properties, it is often necessary to investigate the printing parameters of different substrate materials. In addition, the paths of carbon fibers need to be specially arranged and planned to fully utilize the mechanical properties of carbon fibers. Finally, the denseness of the part needs to be taken into account because of the high porosity of the 3D printed part, which is more serious in FDM. Therefore, the following section summarizes the researchers' studies in three directions: printing paths, parameter settings and the porosity of the fabricated parts.

#### 4.1.1 Printing Path

Samples printed with carbon fibers will show different mechanical properties depending on the orientation of the carbon fibers [69]. In the direction of the carbon fiber print, the carbon fiber parts show the highest tensile strength [70]. For SCFRC, the trajectory of the nozzle affects the orientation of the short carbon fibers, which changes the mechanical properties and failure modes of the component [71, 72]. Yan et al. [73] investigated the effect of the nozzle movement direction on the angle of the short carbon fibers, which provides a basis for controlling the angle of the short carbon fibers. The use of magnetic fields to control the orientation of short carbon fibers is a viable method [74]. For CCFRCs, the setting of the printing path will affect the strength of the CFRC parts and too high the corner will cause the carbon fiber to be misaligned and broken [37]. When 3D printing with continuous carbon fiber prepreg, the number of jumps of the nozzle needs to be controlled, because each jump of the nozzle causes the excess prepreg to be extruded. In addition, if there are too many intersections of paths on the same layer, this can lead to an uneven surface of the carbon fiber part, which can affect the printing result. Therefore, printing parts with high complexity and high mechanical properties with continuous carbon fiber composites remains a huge challenge. At first, the researchers looked to slicing software for inspiration for the design of print paths. Figure 15a to c show three print paths that have been integrated in the FDM slicing software, which are mesh filling, line filling, and spiral filling [69]. Luo et al. [35] experimentally compared the tensile strength of these three filling methods for additively manufactured CCFRC parts, and found that spiral filling was the method to obtain the highest tensile strength. The spiral filling can satisfy the continuous printing of some regular parts, but how to introduce carbon fiber in some irregular and complex parts is still a problem. Analyzing the load transfer path of a component and laying the carbon fiber according to the load transfer path is a new approach to path design. For example, Nakagawa et al. [75] printed tensile specimens in the form of a sandwich, where carbon fibers were neatly laid in the middle layer of the tensile specimen, and the bonding of resin to the middle fibers was enhanced by thermal bonding, as shown in Fig. 15d and e. Li et al. [76] performed a stress analysis of the parts, and placed carbon fibers in the areas of highest stress concentration to improve the mechanical properties of the parts. In this way, the tensile and flexural strengths of the specimens were successfully increased by 67.5% and 62.4%, respectively. The strength of the printed suspension plates was increased by nearly 16 times compared to the pure resin parts. The designed parts and paths are shown in Fig. 15f to j.



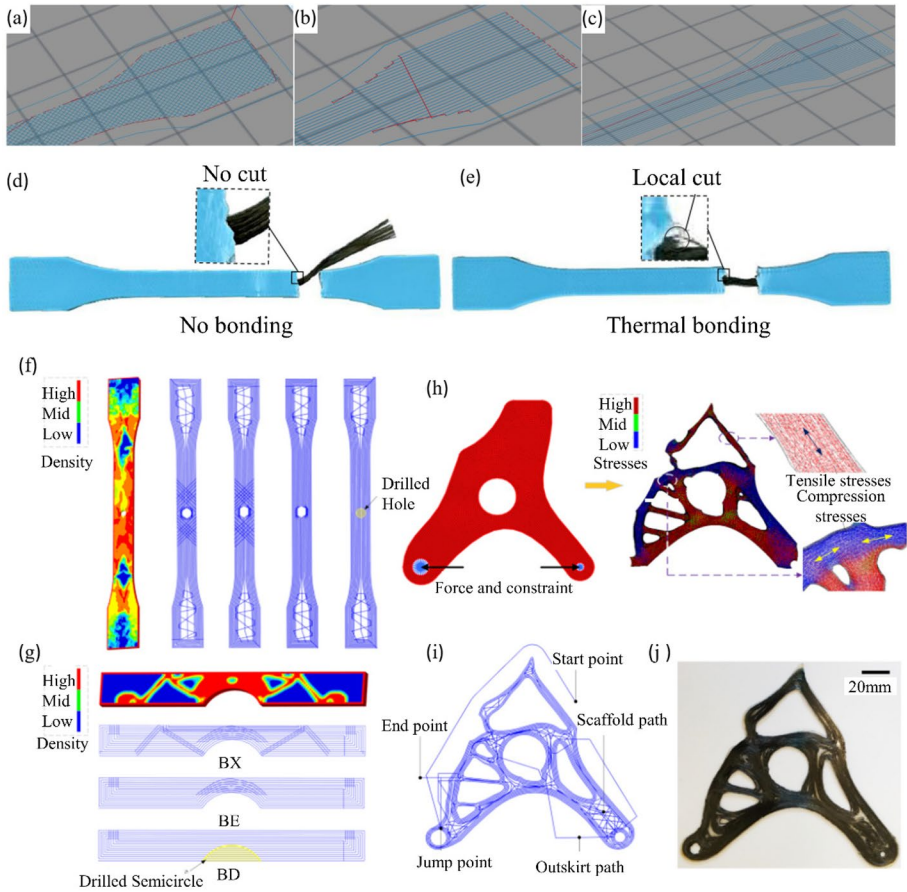


**Fig. 15** Carbon fiber path planning: **a** Mesh filling; **b** Line filling; **c** Spiral filling [35]; **d e** Ruptured tensile specimens without and with thermal heating for  $d=0.4\text{mm}$  [75]; **f** Tension specimen load distribution and printing path; **g** Three-point bending specimen element density and load distribution; **h** Topology analysis of the suspension plate; **i** Hanging plate printing path; **j** Hanging plate printing samples [76]

Path planning for continuous carbon fiber additive manufacturing has been a difficult task for 3D printing high-strength complex parts, and it is difficult to prepare parts with high carbon fiber content in the three ways mentioned above. To obtain parts with high carbon fiber content, it is necessary to use continuous path, while also ensuring that the path does not have too many corners and intersections. Unfortunately, most of all the slicing software currently on the market can only accommodate SCFRCs [77], and even though some scholars have studied continuous fiber paths for AM. For example, Huang et al. [78] proposed an algorithm to optimize tool paths for printing thin-walled honeycomb structures by reducing the number of intersections in the path. These algorithms have not been applied to slicing software [79], and slicing software that can adapt to continuous carbon fiber additive manufacturing has yet to be developed.

#### 4.1.2 Setting of Slicing Parameters

For desktop-level FDM technology, a variety of slicing software is available for download and use. One can change various slicing parameters in the software to complete the slicing of the model and export g-code files for AM. The slicing parameter of the model is the key to the accuracy and mechanical properties of CFRC parts [20, 80, 81]. Yan et al. [82] analyzed the effects of nozzle temperature, print speed and extrusion width on the tensile strength of SCFRC parts. It was shown that there was a direct relationship between the orientation of short carbon fiber and the extrusion width, and the fiber orientation was higher along the printing direction when the extruded filament was narrower. Figure 16a shows the effects of nozzle temperature, printing speed and layer thickness on the tensile strength of SCFRC fabricated parts. The results show that there is no significant positive or negative correlation between these factors and the tensile strength of the fabricated parts. These parameters change the mechanical properties of SCFRC parts mainly by affecting the cooling of the filament, and the mechanical properties of the fabricated part are the result of the coupling of these factors [83]. Figure 16b shows the difference in the tensile strength of the samples with and without the frames. The results show that the frames can improve the tensile strength of the SCFRC fabricated parts to some extent [84].

Dou et al. [85] experimentally studied the effects of the parameter changes of layer height, extrusion width, printing temperature, and printing speed on the mechanical properties of continuous carbon fiber-reinforced PLA composite parts. The results show that

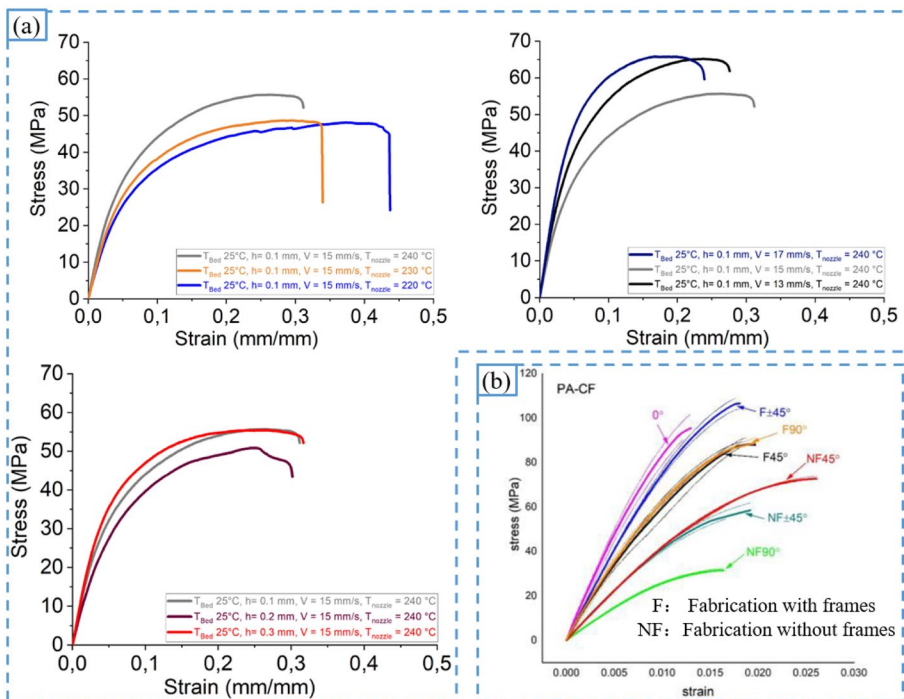


**Fig. 16** Mechanical properties of CFRCs: **a** Effect of slicing parameters on the tensile strength of SCFRC parts by AM [83]; **b** Tensile stress-strain curves for framed and unframed parts [84]

the layer height and extrusion width are negatively correlated with the tensile strength of the parts, while the nozzle temperature and printing speed did not have strict positive or negative correlation with the tensile strength, and could only the optimal solution can only be found in a certain interval. The relationship between these slicing parameters and the tensile strength is shown in Fig. 17a. Similar results were obtained by Jia et al. [86]. The relationship between the tensile strength of the fabricated parts and the layer thickness and printing speed is shown in Fig. 17b. It is noteworthy that both used continuous carbon fiber-reinforced PLA as raw material, but the selection range of layer thickness was not the same, and there is a difference in the maximum tensile strength of the fabricated parts. This is due to the difference in prepreg diameters, and more experiments are needed to determine the process window for different types of FDM equipment and different diameters of prepreg. Figure 17c illustrates the effect of print temperature, print speed, fiber feed and resin feed on the degree of path deviation and fiber kinking. Factor A, B,

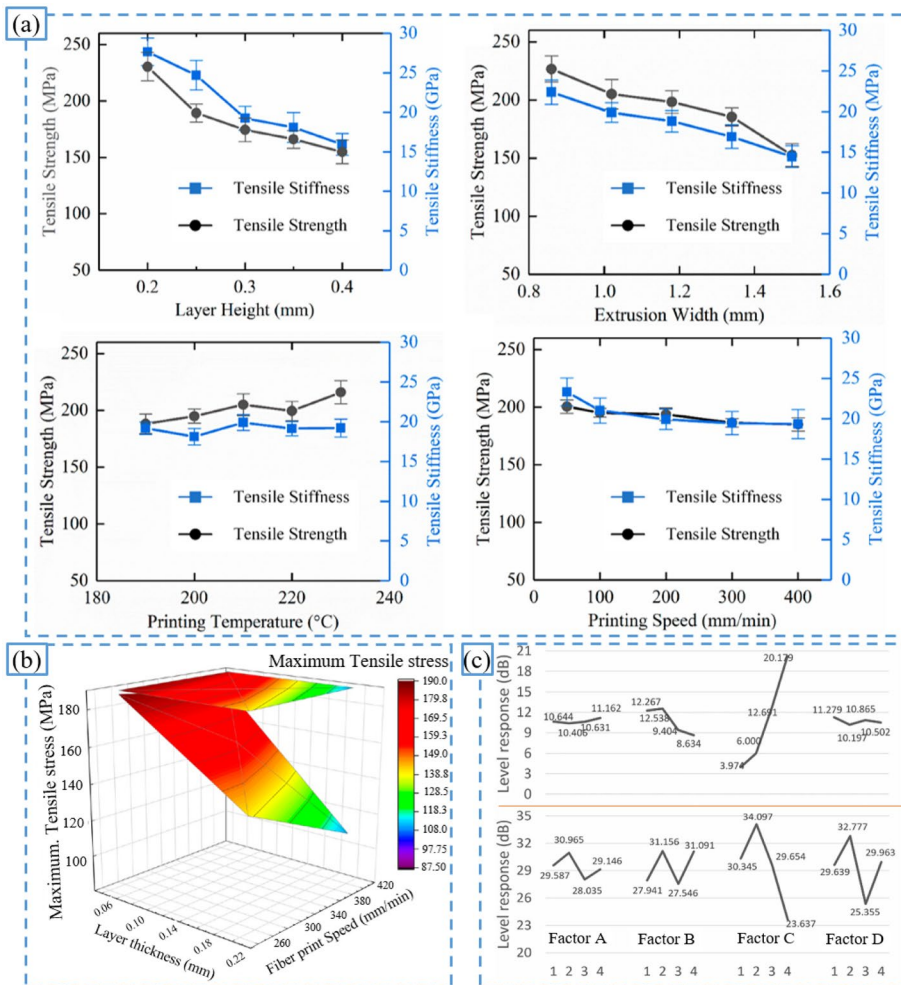


**Fig. 17** Mechanical properties of CFRCs: **a** and **b** Effect of slicing parameters on the tensile strength of CCFRC parts by AM [85, 86]; **c** Effect of slicing parameters on the accuracy of CCFRC parts by AM [87]

C, and D represent print temperature, print speed, fiber feed, and resin feed, respectively. The results show that printing speed and fiber feed rate have a significant effect on the accuracy of the part [87].

Finally, for laser-assisted in-situ curing additive manufacturing methods, the irradiation power of the laser has a significant impact on the mechanical properties of the manufactured part [88].

The study of slicing parameters is the most fundamental issue in continuous carbon fiber additive manufacturing, and some conclusions can be drawn from the above studies:

1. The main parameters that affect the accuracy of the fabricated parts are filling path, printing speed, nozzle temperature, and diameter. The influence of the filling path on the accuracy is mainly reflected in the unevenness of the part caused by the intersection of the path. Too fast a printing speed can cause the carbon fiber to be pulled out at the corners. The temperature of the nozzle will affect the fluidity of the resin. High temperature will make the previous layer melt again and low temperature will make it difficult to fuse the resin between the two adjacent lines, thus forming defects. Finally, the diameter of the nozzle needs to be matched to the diameter of the prepreg.
2. The key factors affecting the mechanical properties of the continuous carbon fiber additive manufacturing parts are the path, layer thickness, and scan spacing. The influence of the path on the mechanical properties of the continuous carbon fiber additive manufacturing parts has been discussed in the previous chapter, while the layer thickness and scan spacing needs to be selected according to the diameter of the prepreg. By changing these two parameters, parts with different porosity which affects the mechanical properties of the parts can be obtained.

### 4.1.3 Porosity

Compared to traditional compression forming processes, CFRC parts using AM as a forming method have higher porosity, which is an important factor in the mechanical properties of the parts [89]. When manufacturing CFRC parts with FDM, the nozzle diameter is usually larger than the prepreg diameter. Larger nozzle diameters create more air pockets in smaller sized corner areas [90, 91]. An increase in the volume fraction of carbon fibers leads to a decrease in the volume fraction of resin. When the resin content is not sufficient to supply fiber-to-fiber bonding, the porosity inside the manufactured part rises [91, 92].

For SCFRC parts, Lin et al. [93] prepared SCFRC parts with different carbon fiber volume fractions and investigated the effect of carbon fiber volume fraction on the mechanical properties of the parts. The results showed that the flexural strength of the SCFRC parts reached the highest when the volume fraction of carbon fiber reached 3.5%-4.5%. Young's modulus of the SCFRC parts reached the highest when the carbon fiber volume fraction was 6%. As the volume content of carbon fiber continued to increase, the flexural strength and Young's modulus both decreased. As can be observed from Fig. 18a to c, the higher the carbon fiber content, the higher the porosity of the fabricated parts. To investigate the mechanism of pore formation inside the fabricated parts, Somireddy et al. [94] investigated the relationship between porosity and mechanical properties of SCFRC components at different layer thicknesses. This study shows that choosing the right layer thickness can be effective in reducing the porosity

within the composite. The smaller the layer thickness, the higher the pressure of the printer nozzle on the composite filament. Under high pressure, the resin is more easily squeezed into the fiber filaments, which in turn reduces the porosity of the manufactured part. Yang et al. [95] investigated the evolution of short carbon fibers and pores during 3D printing. They found that the porosity of the composite filament inside the nozzle is low and most of the pores are formed when the composite filament leaves the nozzle, and Fig. 18f to i shows the process. Nozzle shape is also an external factor that affects part porosity. As shown in Fig. 18d and e, the square nozzle printed sample porosity is lower than the sample printed by the circular nozzle [96].

For CCFRC parts, the carbon fibers can come into contact with the surface of the processing equipment and break, which can exacerbate the formation of pores. The print path also has an effect on the porosity of the part [82, 89, 97]. He et al. [98] prepared continuous carbon fiber-reinforced nylon composites, observed the part's cross-sectional pores using optical microscopy, and reduced the porosity inside the part by molding. Figure 18j to m shows the difference in porosity between the compression and non-compression molding. In addition, Li et al. [99] investigated the effects of fiber volume fraction, fiber shape and fiber eccentricity on the on the printing process through numerical simulations. Based on this study, it is expected to further understand the causes of porosity formation in additive manufacturing process and regulate it.

In summary, the source of pores in additively manufactured CFRC parts can be divided into these components:

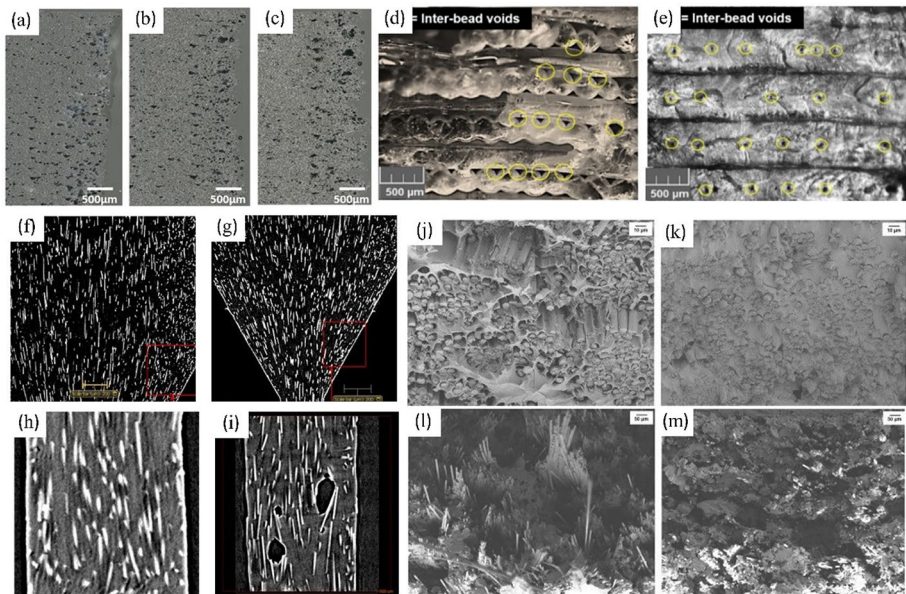


**Fig. 18** SEM of parts with different carbon fiber content: **a** 10% **b** 20% **c** 30% [89]; SEM of printed parts with different shaped nozzles: **d** circular nozzle **e** square nozzle [96, 98]; CT of carbon fiber extrusion process: **f** in the chamber **g** at the nozzle **h** at the nozzle outlet **i** completely out of the nozzle [95]; Fracture surfaces of bending specimens printed with CFRCs: **j** and **k** with compression molding **l** and **m** non-compression molding [98]

1. In the preparation of prepreg, the incomplete contact between resin and carbon fiber leads to a raw material with high porosity. As a result, porosity is more likely to occur during the preparation of SCFRCs compared to CCFRCs.
2. During additive manufacturing, sharp rotation and jumping of the nozzle increases the porosity of the manufactured part. The use of appropriate slicing parameters and path planning can alleviate this problem to some extent.
3. The internal roughness of the nozzle affects the condition of the carbon fiber filament as it leaves the nozzle. Excessive roughness will cause the prepreg to become more porous as it leaves the nozzle. Smoothing the inside of the nozzle helps to feed the prepreg neatly and evenly through the nozzle, thereby reducing porosity in the manufactured part.

## 4.2 Comparison of Short Fiber and Continuous Fiber-reinforced Composite

### 4.2.1 The Influence of Fiber Form on the Part

Unlike continuous carbon fiber, short carbon fibers only provide local reinforcement to the composite filaments. When carbon fibers are ground into powder form, the mechanical properties of thermoplastic composite parts are not significantly improved [100, 101]. Figure 19 illustrates the difference in mechanical properties between SCFRC fabricated parts and CCFRC fabricated parts. Figure 19a and b verify the relationship between the above-mentioned short carbon fiber content and the mechanical properties of the parts, the content of short carbon fibers needs to be controlled within a certain range to obtain the highest mechanical properties of the parts. Figure 19c and d show the tensile strength and flexural strength of the CCFRC parts, respectively. By comparing the mechanical properties of SCFRC and CCFRC fabricated parts, it can be concluded that continuous carbon fiber strengthens the parts more effectively. Hao et al. [49] also proved this conclusion.

The distribution of pores and the reasons for their formation are also different for SCFRC and CCFRC parts. Figure 20a to h shows the pores of the SCFRCs, and it can be seen that many pores are present around the short carbon fibers [14]. The bonding of continuous carbon fibers to the matrix occurs mainly in the form of the matrix wrapping around the carbon fiber tows. Excellent impregnation results depend on the ability of the matrix to penetrate the carbon fiber tow so that each carbon fiber monofilament is coated with the matrix. As the fiber content increases, the matrix wrapping effect will become less and less effective. When the continuous carbon fiber content is low to a certain extent, the matrix will be difficult to penetrate the carbon fiber bundle, and the phenomenon of fiber and matrix separation occurs [104]. This phenomenon can be seen in Fig. 20i to l.

The current FDM technology also realizes the printing of continuous fibers, but the printing process will inevitably cause certain damage to continuous fibers [90, 105]. When printing CCFRC parts, the equipment requirements are more demanding, as the continuous fibers are more likely to wear out from contact with the printing equipment during the printing process [49]. This problem does not occur when printing SCFRC parts. Hu [102] monitor the continuous fiber FDM printing process. As shown in Fig. 20m to o, the modal transformation of the continuous fibers mainly occurs when it is pulled out of the drum and when it is extruded from the nozzle. Carbon fiber is heated and softened as it passes through the printer nozzles, and the surface is abraded as it passes through the pulleys and rollers. Because of this, a large number of breaks occur in the continuous carbon fiber as it is laid on the printing plate. Figure 20s and t shows the fracture of continuous carbon fiber after different diameters of the nozzle end. It can be seen that the reduction of the nozzle

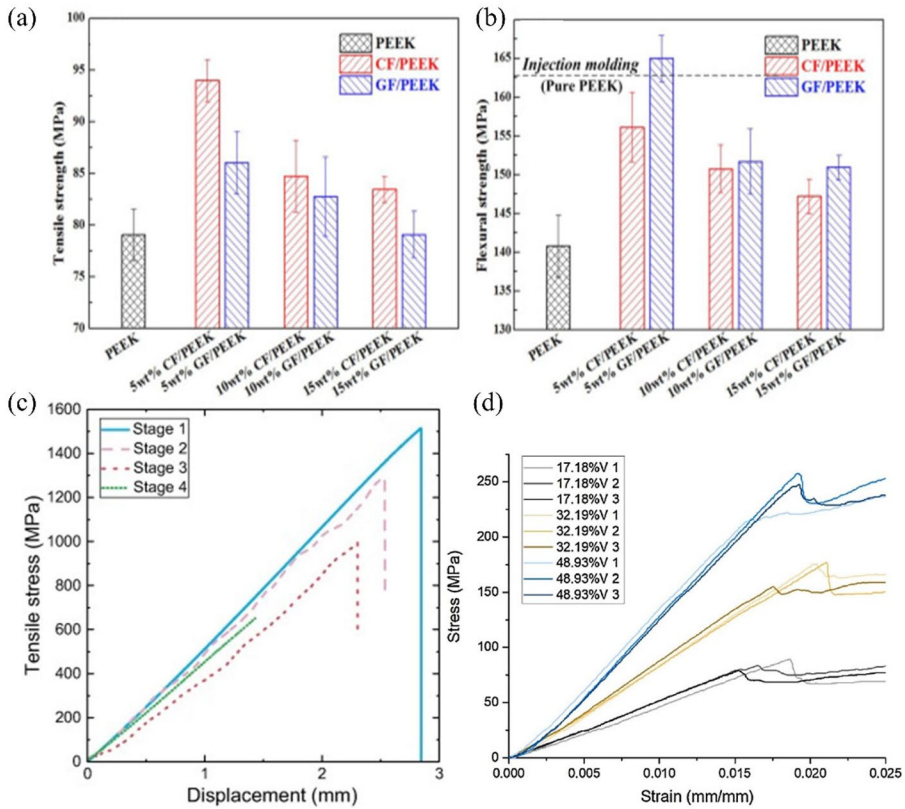


**Fig. 19** Mechanical properties of short fiber-reinforced PEEK parts [14]: **a** Tensile strength **b** Flexural strength **c** Tensile strength of continuous fiber-reinforced polyamide parts [102]; **d** Flexural strength of carbon fiber-reinforced PA6 parts with different carbon fiber content [103]

diameter exacerbates continuous fiber fracture, whereas short carbon fibers are insensitive to nozzle diameter [47].

#### 4.2.2 The Influence of the Matrix on the Part

Depending on the molecular structure, the matrix of fiber-reinforced composites can be classified as thermosetting polymers or thermoplastic polymers. Thermoplastic resins include ABS, PLA, PETG, PEEK and nylon [106–108]. Thermoplastic polymers have no chemical cross-linking and have good physical and mechanical properties at characteristic temperatures. Because of their ease of processing, they are the most commonly used substrates for FDM [40, 109]. Thermoplastic polymers are prone to warpage during the printing process. Warpage is influenced by the crystallinity of the thermoplastic polymer material, the lower the crystallinity, the less warpage and the more accurate the dimensional control [110]. Ambient temperature is a key factor affecting crystallinity. Yang et al. [111] varied the ambient temperature to control and achieve different crystallinity of PEEK components. The results show that pure PEEK undergoes a non-isothermal crystallization process when extruded from the nozzle. The ambient temperature setting adds

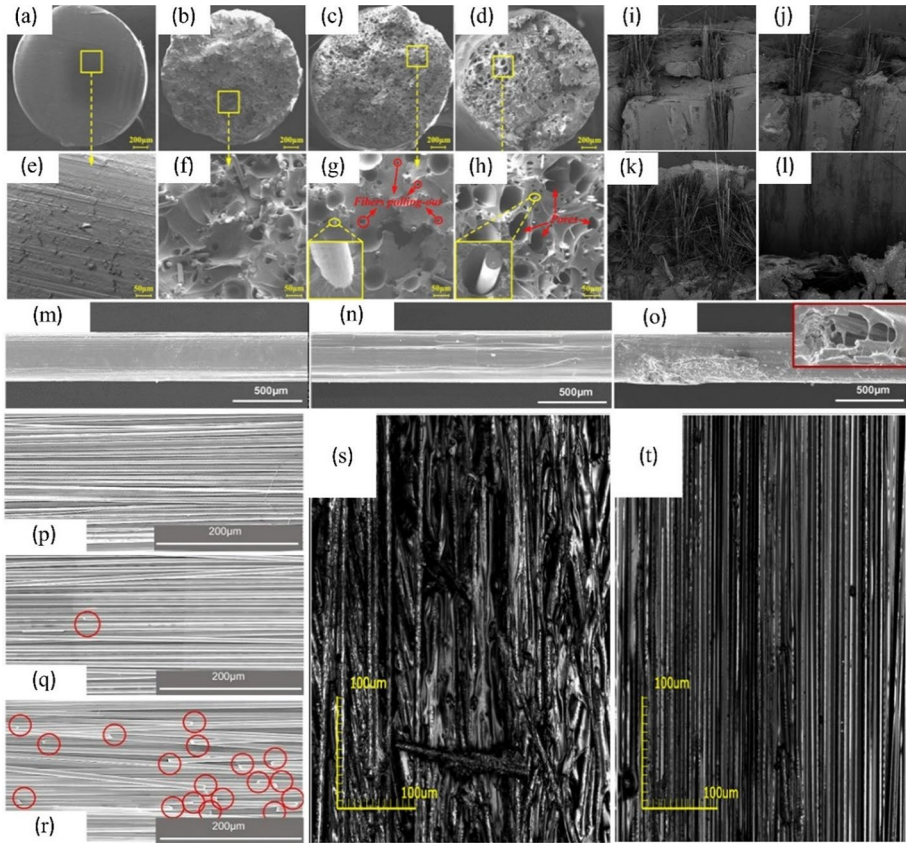


**Fig. 20** SEM of filament cross-section with different short fiber content: **a** and **e** 0wt% **b** and **f** 5wt% **c** and **g** 10wt% **d** and **h** 15wt% [14]; SEM of different continuous fiber content: **i** 3wt% **j** 5wt% **k** 10wt% **l** 15wt% [104]; the Surface texture of the FDM filament at stages: **m** Raw feedstock **n** Through two counter-rotating metal wheels **o** Through heating element 254 °C; Longitudinal images of the FDM filament in stages: **p** Raw feedstock **q** Through two counter-rotating metal wheels **r** Flattened by heated nozzle on an unheated bed 20 °C [102]; The surface of the filament impregnated with nozzles of different diameters: **s** 0.6 mm **t** 1.0 mm [47]

an isothermal crystallization process to the extruded polyether ether ketone, with a corresponding increase in the crystallinity of pure polyether ether ketone from 17 to 31% as the temperature rises from 25 °C to 200 °C. The crystallinity of the extruded polyether ether ketone increases from 17 to 31% as the temperature rises from 25 °C to 200 °C. This conclusion is shown in Fig. 21a and b. Figure 21c and d shows the results of crystallinity and mechanical properties of different PEEK samples at different nozzle temperatures. Yang [13] measured the crystallinity and warpage of carbon fiber-reinforced PEEK composite parts prepared by FDM at different ambient temperatures. The results show that the law of influence of ambient temperature on crystallinity is also applicable to the AM of short carbon fiber-reinforced PEEK. As seen in Fig. 21e, the crystallinity of carbon fiber-reinforced PEEK gradually increases from 21.3% to 32.5% as the temperature increases from 20 °C to 200 °C, and the warpage of the fabricated parts first increases from 0.2% to 1.6% and then decreases to 0.4%. The reason for the decrease in warpage is that when the temperature is



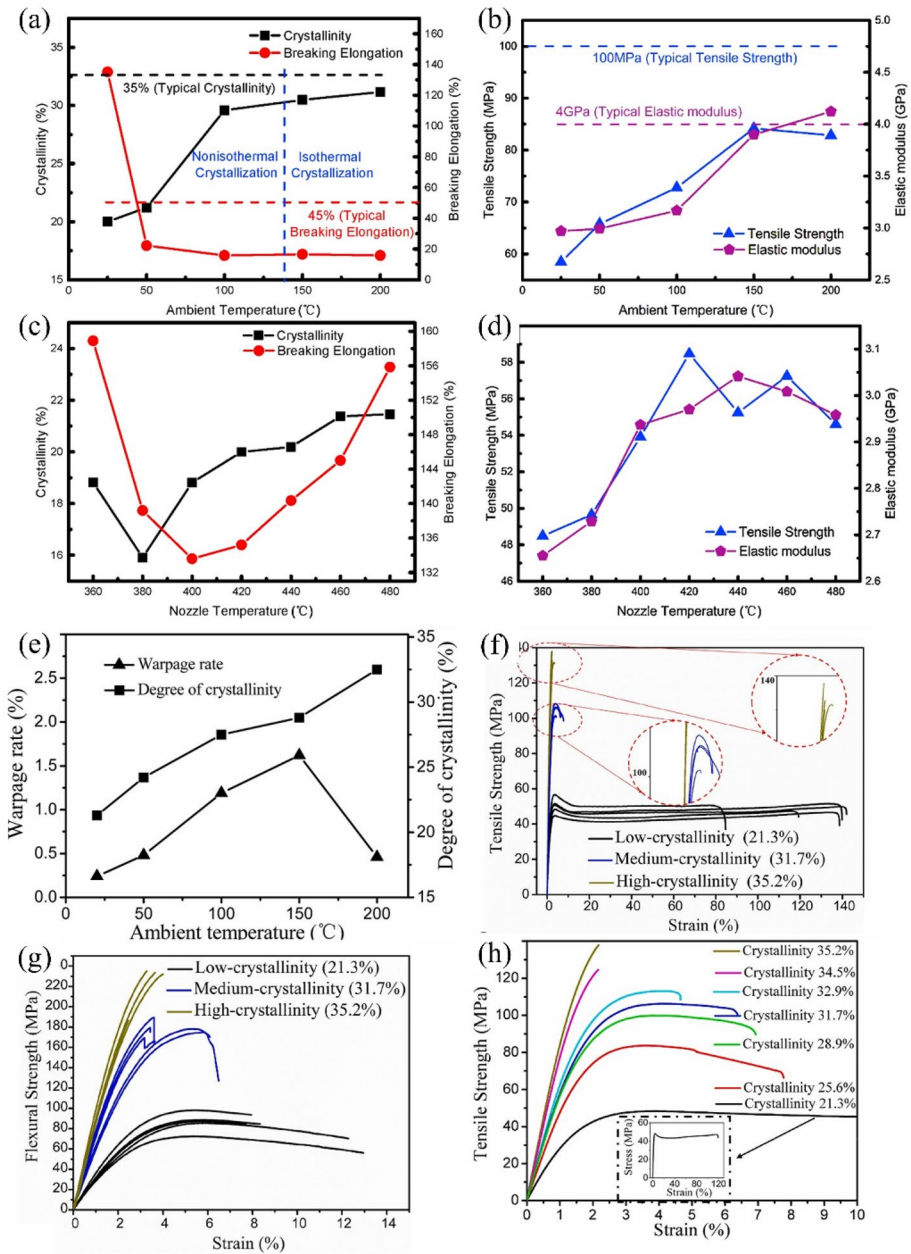


**Fig. 21** Crystallinity and mechanical properties results of different PEEK samples with different ambient temperatures (25 °C, 50 °C, 100 °C, 150 °C, 200 °C): **a** results of crystallinity and breaking elongation **b** results of tensile strength and elastic modulus; Crystallinity and mechanical properties results of different PEEK samples with different ambient temperatures (360 °C, 380 °C, 400 °C, 420 °C, 440 °C, 460 °C, 480 °C): **c** results of crystallinity and breaking elongation **d** results of tensile strength and elastic modulus [111]; **e** Effects of ambient temperature on crystallinity and warpage rate of carbon fiber-reinforced PEEK composite parts prepared by the FDM process; **f** and **g** Relationship between the crystallinity and tensile stress–strain curves and flexural stress–strain curves of carbon fiber-reinforced PEEK composite samples after heat. **h** Control of mechanical properties of the carbon fiber-reinforced PEEK composite through recrystallization [13]

at 200 °C, the composite part changes from non-isothermal to isothermal crystallization, the ambient temperature is higher, and the part presents a semi-softened state, thus less shrinkage and deformation occurs. The mechanical properties and elongation of carbon fiber reinforced PEEK composites can be controlled by varying the FDM process parameters and the crystallinity of the composite post-treatment, as shown in Fig. 21f to h. However, it is worth noting that the elongation of the composites is more sensitive to crystallinity. Therefore, processes that allow better control of crystallinity are needed.

The molecules of thermoset resin cross-link during curing to form a mesh structure, so the thermoset resin has the characteristics of rigidity, high hardness, high-temperature resistance and non-flammability after curing [112]. The difficulty of molding thermoset resins in FDM is one of the reasons why there is less research on this material than on thermoplastic resins. As equipment is updated and technology matures, the advantages of thermoset resin materials in 3D printing are gradually revealed [113]. AM of carbon fiber-reinforced thermoset resins typically uses a lasers to cure the resin, which requires precise control of the laser’s irradiation angle, power and exposure time. At present, there are few studies on the bonding quality of thermoset resins to carbon fibers, and the mechanism of heat-force-flow coupling of carbon fiber-reinforced thermoset resins under the AM process is still to be explored.

### 4.2.3 Discussion of Failure Modes of CCFRC Parts

The tensile fracture forms of CCFRC parts mainly include fiber pull-out, fiber debonding, and fiber breakage [114]. As shown in Fig. 22a. Fiber debonding and fiber pullout are mainly caused by poor bonding between matrix and fibers due to pores created during the

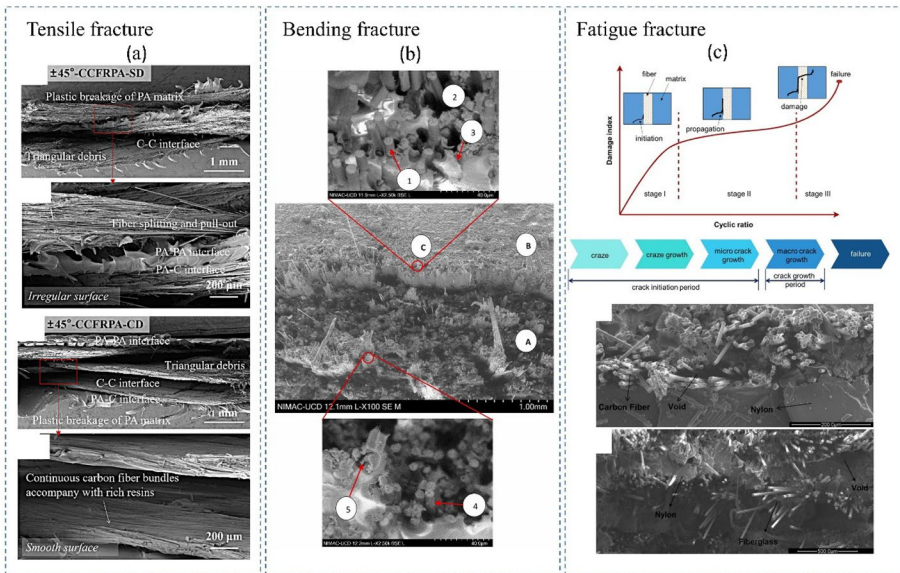


**Fig. 22** Failure modes of CCFRCs: **a** SEM image of fracture surface after stretching [116]; **b** SEM image of the fracture surface after bending [117]; **c** Fatigue failure process and typical fatigue fracture surface SEM images of CCFRCs [115, 118]

manufacturing process, and these two failure modes are dominated by the matrix. Fiber fracture is the failure mode that can withstand the maximum tensile stress, and this failure mode is mainly caused by the propagation of micro cracks on the surface of the carbon fiber. Figure 22b shows the bending fracture cross-section of CCFRC parts. It can be seen that the damage form in zone A is the same as the tensile damage form, with the neutral plane (C) flanked by tensile (A) and compressive (B) sides, respectively. The fracture surface in zone B looks more dense and flat, which is caused by the extrusion of the matrix. Figure 22c shows the failure mechanism of the CCFRCs. Failure of CCFRCs can be divided into three stages. The initial stage of failure is related to the debonding of the fiber matrix in areas where poor bonding exists, poor bonding is due to fiber misalignment, matrix enrichment, and poor surface conditions. In the second stage, delamination occurs between the fibers and the matrix. In the final stage, crack extension occurs in the fibers and local fracture occurs [10]. Carbon fiber-reinforced thermoplastic composites fail more commonly in the first stage, whereas thermoset resins form a higher quality bond with the fibers after curing and can pass through the first stage more smoothly [115].

### 4.3 Key Factors of SLS Forming Quality

#### 4.3.1 Fiber Orientation

When printing pure polymers by SLS, the mechanical anisotropy of the printed sample is relatively low, but with the addition of carbon fibers, the anisotropy of the parts becomes noticeable [119–121]. The tensile strength of the part is significantly improved along the fiber, but the elongation is also decreases significantly [57]. The reduction in elongation is clearly shown in Fig. 23a and b. Figure 23c and d show the relationship between carbon fiber orientation, porosity and carbon fiber content of short carbon fiber polymer parts, respectively. The strength of CFRC parts increases significantly in the direction of carbon fiber alignment, remains almost unchanged perpendicular to the direction of carbon fiber alignment, and decreases slightly perpendicular to the interlayer direction. The main reason for the decrease in strength perpendicular to the interlayer direction is that the porosity of the interlayer increases with the addition of rigid carbon fibers [122]. Khudiakova et al. [121] used X-ray computed tomography and characterized the structural characteristics of carbon fiber-polyamide 12 composites processed with SLS. The results showed that most of the carbon fibers were laid in a direction parallel to the block direction. There are three factors that increase the shear force of carbon fiber by the squeegee: an increase in squeegee travel speed, an increase in squeegee rotation speed and a decrease in layer thickness. These three factors because more carbon fibers to be aligned parallel to the direction of powder lay-up, thus improving the tensile properties of the carbon fiber composite product in the powder lay-up direction. Chen et al. [123] monitored the orientation changes of carbon fibers during the preparation of short carbon fiber polymer parts by SLS and simulated the role of powder diffusion in the formation of fiber orientation by the discrete element method. As shown in Fig. 23e to g, the mixture exhibits highly heterogeneous morphology and size distribution. The torque generated during powder spreading process causes the carbon fibers to rotate in the spreading direction, which is generated by the shear flow influenced by the layer thickness, spreading speed and the rotational speed of the rollers.

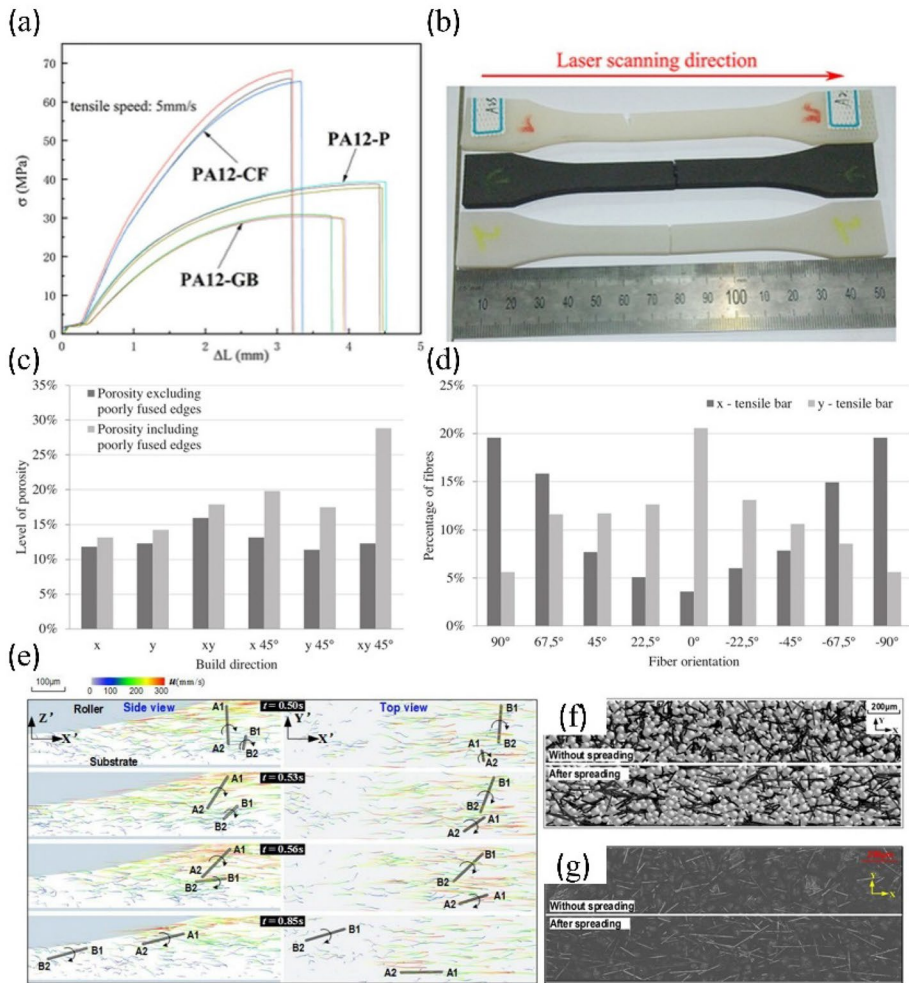


**Fig. 23** Effect of fiber orientation on mechanical properties of fabricated parts: **a** Carbon fiber-reinforced PA12 parts by SLS (PA12-CF), glass beads-reinforced PA12 parts (PA12-GB) by SLS, and pure PA12 parts SLS stress deformation curve; **b** PA12-P, PA12-CF, PA12-GB specimen fracture diagram (from top to bottom) [57]; **c** The porosity of carbon fiber-reinforced PA12 parts by SLS; **d** The different orientation content rates of carbon fibers in x- and y-oriented tensile specimens, 90° and 0° are parallel to and perpendicular to the construction direction of the specimen, respectively [122]; **e** The formation process of fiber orientation during powder diffusion; **f** DEM simulation diagram; **g** SLS experimental electron microscopy diagram [123]

### 4.3.2 Parameters

The process parameters of SLS include laser power, laser speed, hatch spacing, layer thickness, preheating temperature, and printing direction, and the setting of different parameters will have an impact on the accuracy of sample forming and the mechanical properties after forming [124, 125]. Czelusniak et al. [126] investigated the effect of laser energy density on the mechanical properties of carbon fiber-reinforced PA12 parts fabricated by SLS. The density, elastic stress, modulus of elasticity, plastic stress, and nominal strain of the

printed part increase with increasing energy density. As shown in Fig. 24a, the density and mechanical properties of the part reach a maximum when the energy density reaches about  $0.181 \text{ J/mm}^3$ , and begin to decrease as the energy density continues to increase. The reason for this result is that higher energy densities lead to thermal degradation of the oxygen groups on the surface of the carbon fiber during the printing process and their release into gases, which increases the porosity of the part and consequently leads to changes in the mechanical properties of the part. Figure 24c and d demonstrate similar conclusions [127].

The mechanical properties of the carbon fiber-reinforced composite parts prepared by the SLS are affected by the orientation of the carbon fibers, the modified additives, and various process parameters. The relationship between these parameters and the mechanical properties of the carbon fiber fabricated parts is demonstrated in Fig. 25a to d. Appropriately increasing the laser power can effectively improve the tensile strength and modulus of SCFRC parts, but the mechanical properties of the parts begin to decrease when the laser power exceeds 19W. This is consistent with the trend depicted in Fig. 25a. The layer thickness has a significant effect on the tensile strength of the SCFRC, and the tensile strength of the sample with a layer thickness of 0.1 mm is more than twice that of the sample with a layer thickness of 0.15 mm. The tensile strength and modulus are optimal at a carbon fiber mass fraction of 10% and are significantly higher than those of the sintered pure PEEK parts. When the carbon fiber content is greater than 10 wt%, the enhancement is mainly in the tensile modulus. The composites with 15 wt% and 20 wt% carbon fiber content had lower tensile strength than pure PEEK. The composites with different carbon fiber contents show similar patterns in bending strength and modulus [53]. As shown in Fig. 25e and f,

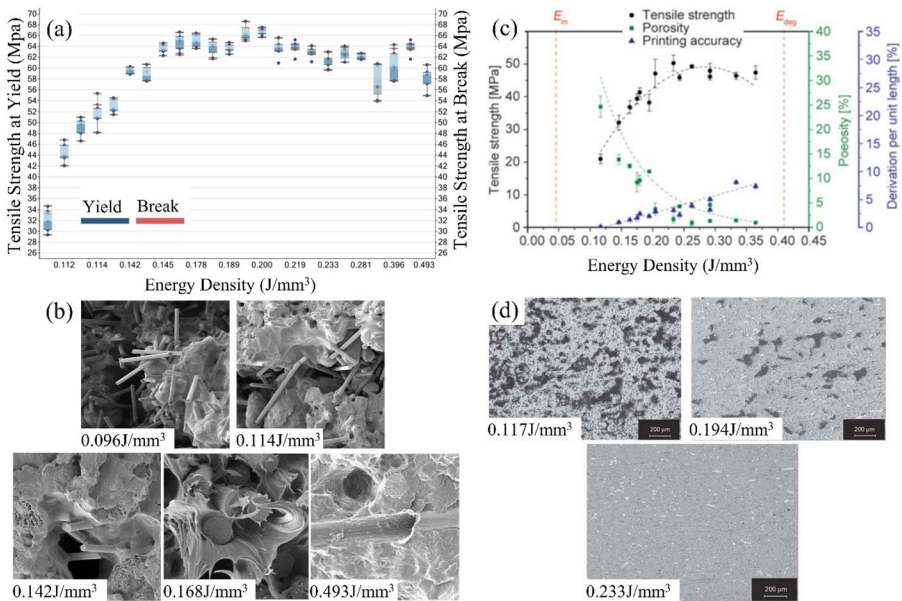


**Fig. 24** Mechanical properties and cross-section characterization of CFRC fabricated parts: **a** Effect of energy density on tensile strength of CCFRC parts; **b** SEM micrographs of CCFRC parts at different energy densities [126]; **c** Effect of energy density on tensile strength, porosity, and accuracy of CCFRC parts **d** SEM micrographs of CCFRC parts at different energy densities [127]

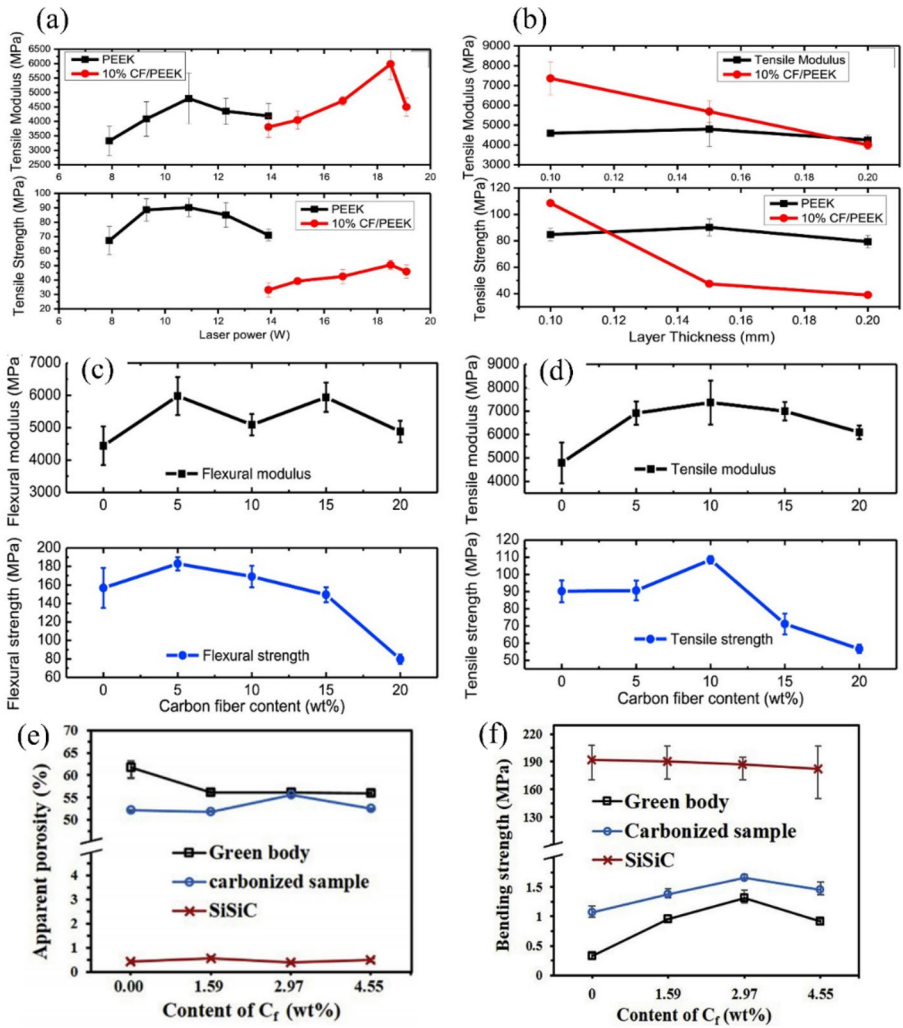


**Fig. 25** The tensile modulus and strength of PEEK and composites with 10wt% CF VS laser power: **a** The laser power of 18.5 W for CF/PEEK and 10.9 W for pure PEEK **b** The layer thickness of 0.1 mm to 0.2 mm; **c** and **d** Mechanical strengths VS CF content (process parameters: laser power of 18.5 W, layer thickness of 0.1 mm) [53]; **e** Relationship between the volume fraction of carbon fibers and the porosity content of their fabricated parts; **f** Relationship between volume fraction of carbon fibers and flexural strength of their fabricated parts [58].

the Green body, Carbonized sample, and SiSiC denote the initially printed CFRC part, the sintered CFRC part, and the silicon infiltrated part, respectively. The incorporation of a moderate amount of carbon fibers improved the mechanical properties of the raw and carbonized sample but did not improve the mechanical properties of the final SiSiC samples. In general, the addition of carbon fiber does improve the mechanical properties of the part, but it is not that adding more carbon fiber is better. Better control of the orientation of the carbon fibers will better demonstrate the reinforcing properties of the carbon fibers [58].

## 5 Applications

### 5.1 Biomedical Engineering

Due to the advantages of personalization and rapid prototyping, AM is particularly suitable for application in the medical field. For example surgical assistance, personalized medical device printing, tissue engineering, medical education, and basic science research [128]. At present, there have been cases of CFRCs as implant materials *in vivo*. The use of carbon fiber composites as *in vivo* implants has the advantages of radiological diagnosis and treatment [129, 130]. As shown in Fig. 26, Alia et al. [131] designed a novel carbon fiber reinforced polymer orthosis for supporting the posterior calf to assist in the treatment of patients with foot drop disorders. Marinopoulos has also successfully developed a 3D printed carbon fiber-reinforced nylon prosthetic receiving chamber [132]. Furthermore, The addition of carbon fiber can improve the mechanical properties of biomaterials [133]. For instance, PEEK is a biocompatible material compared to other polymers, but its strength limits its use in orthopedic implants compared to metallic materials (Ti). Han et al. [134] conducted research on the biocompatibility of carbon fiber-reinforced PEEK composites and successfully printed the sternum and nasal bone with FDM. The results show that carbon fiber-reinforced PEEK composites with appropriate mechanical strength have the potential to act as biomaterials for bone grafting and tissue engineering applications. Moreover, Carbon fiber has excellent electrical conductivity and can be used to make sensing equipment. Davoodi et al. [135] printed a flexible piezoresistive composite sensor with carbon fiber. The sensor is highly flexible, foldable and electrically sensitive. It can be used to detect human joint movements and biological signals.

### 5.2 Aerospace Engineering

In recent years, drones have become increasingly popular in the military, private, and public sectors due to the shorter take-off distances, longer flight endurance, and lighter construction. Traditional manufacturing methods make it difficult to create lightweight structures with complex internal structural features, but AM can be easily achieved [136]. As

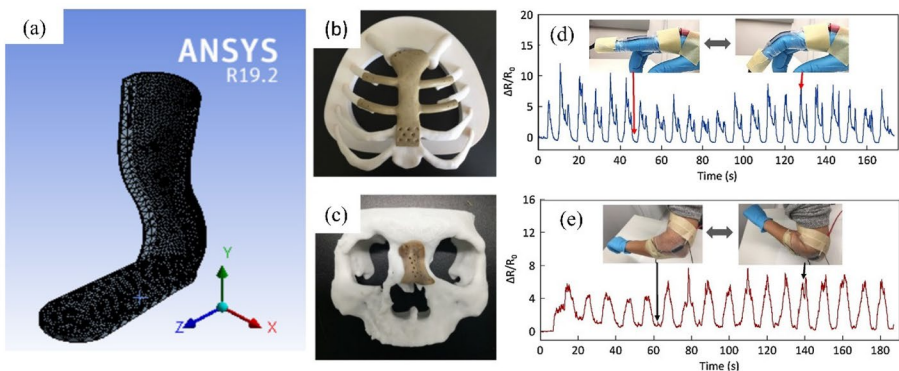


**Fig. 26** Application of CFRCs in medical engineering: **a** Carbon fiber-reinforced polymer orthosis [131]; **b** Additively manufactured PEEK sternum **c** Additively manufactured PEEK nasal bone [134]; **d** Index finger motion detection sensor **e** Elbow motion detection sensors [135]

shown in Fig. 27a to c, Azarov et al. [137] printed a small drone frame using CFRCs with a mass of only 75g, while existing drone frames with similar dimensions range from 130 to 230 g. Saputro et al. [138] printed a racing quadcopter with carbon fiber-reinforced PLA composites through the method of structural optimization, the aircraft has a lighter mass and maintains the original stiffness.

For large passenger aircraft, CFRCs play a significant role in lightweight design. As shown in Fig. 27d to i, AM is used for many CFRC parts of aircraft. AREVO successfully designed and printed hinged brackets and seat brackets for passenger aircraft, replacing traditional metal with CFRCs, reducing the weight of hinged brackets by 70% and eliminating unnecessary tails on the structure. The seat bracket has been reduced from four aluminum parts to one carbon fiber-reinforced lightweight part, resulting in a 30% weight reduction.

### 5.3 Living and Traveling

CFRCs can be found everywhere in our lives, and the casting process of using CFRC to manufacture sports equipment has matured and is widely used in practice. Additive manufacturing pays more attention to personalized customized content. Some businesses use AM to provide one-on-one manufacturing services to their customers. Figure 28 illustrates various CFRC components prepared by AM. A typical bicycle is made of hundreds of

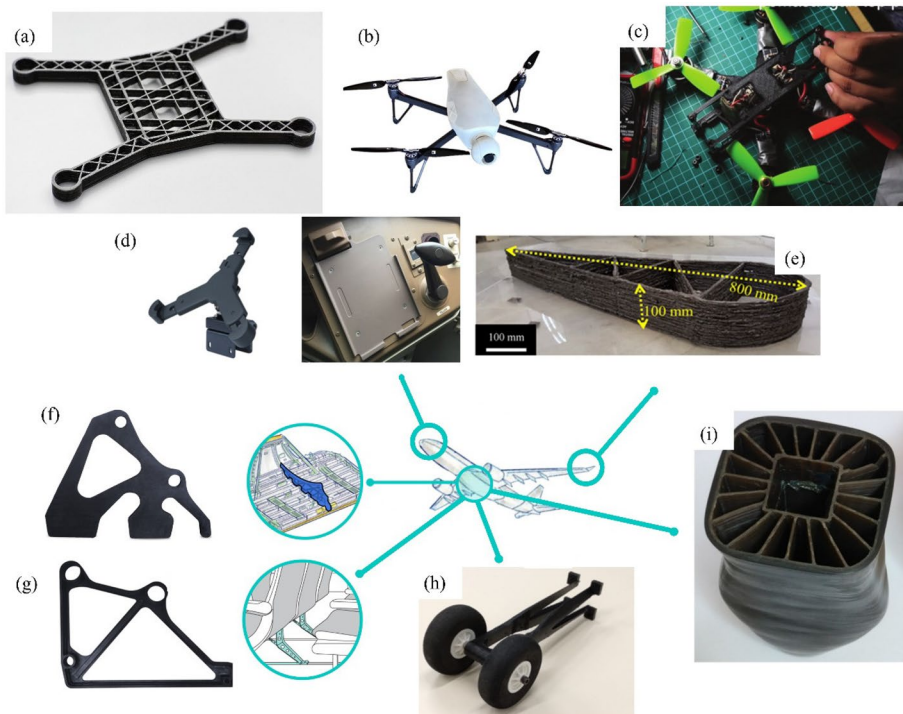


**Fig. 27** CFRCs in aerospace applications: **a** Additive manufactured small drone frame with CFRCs [137]; **b** and **c** Small drones carrying additive manufactured CFRC frame [138]; **d** Cockpit "Electronic Flight Packet" bracket; **e** Wing ribs printed with CCFRCs [100]; **f** and **g** Hinge brackets and seat brackets for large airliners; **h** Aircraft landing gear printed with CFRCs [9]; **i** UAV complex core structure by FDM [136]





**Fig. 28** Additive manufacturing products with CFRCs [62]

bonded and bolted parts. However, through additive manufacturing, it is possible to create a truly one-piece bicycle frame. Using the high strength-to-weight ratio of carbon fiber, lighter weight e-bikes can be printed. The unique path design maximizes the capabilities of carbon fiber composites. In terms of automotive light-weighting, additive manufacturing of CFRCs shows stronger advantages. Examples include carbon fiber wheel hubs, car trunks, and customized interior seats. In sports, bespoke carbon fiber sports equipment can better meet the training needs of athletes.

## 5.4 Honeycomb and Sandwich Construction

Lightweight structures with high energy-absorbing capacity are becoming increasingly popular in aerospace, transportation, and shipbuilding. Honeycomb structures, as a leader in lightweight structures, have been used in these fields [139]. CCFRC have a unique advantage in preparing honeycomb structures. Honeycomb panels consist of an upper and lower skin and a structural sandwich. Fiber-reinforced composites can be used in any part of the honeycomb panel. As shown in Fig. 29a, the top and bottom skins of the honeycomb panel are made of CCFRCs, while the core layer is achieved by FDM using SCFRCs [140, 141]. CCFRCs can also be utilized to prepare the core layer of honeycomb panels. As shown in Fig. 29b, if CCFRCs are utilized to prepare the core layer of honeycomb panels, the pathway needs to be carefully designed to meet the manufacturing requirements. This has the advantage of achieving a higher specific energy absorption capacity than aluminum alloys [142].

In addition to conventional two-dimensional honeycomb structures, three-dimensional structural sandwiches pose greater challenges for AM. As shown in Fig. 29c and d, these sandwich structures are not stretched from a particular face, but are usually made of individual parts joined by adhesive gluing and welding. These methods can lead to defects at the joints of the sandwich structure [143]. Currently, the printing of these sandwich structures can only be realized using SCFRC through the SLS process. It is still a challenge to additively manufacture these structures with CCFRC [144].

## 5.5 4D Printing

4D printing technology is a potential manufacturing process for lightweight, high-strength smart composite structures that can be used to create materials. Active materials are capable of being activated controllably by environmental stimuli and changing conformation over time, and CFRC is one such material [145]. Zeng et al. [146] fabricated continuous carbon fiber reinforced shape memory PLA composite parts using FDM and bent them. As shown in Fig. 30a, the shape recovery of the fabricated part after resistive heating is greater than 95%, and the CCFRCs fabricated by 4D printing can be used as electrically actuated and controllable potential components. Dong et al. [147] proposed a strategy for fabricating intelligent carbon fiber-reinforced lattice structures based on cold programming-induced shape memory effect. Negative Poisson's ratio structures printed by this strategy 4D (Fig. 30b) can not only dissipate a large amount of energy, but also recover to the original shape after being stimulated. A similar structure (Fig. 30d) is the hypersurface chiral structure with electromagnetic frequency selectivity and isotropy designed by

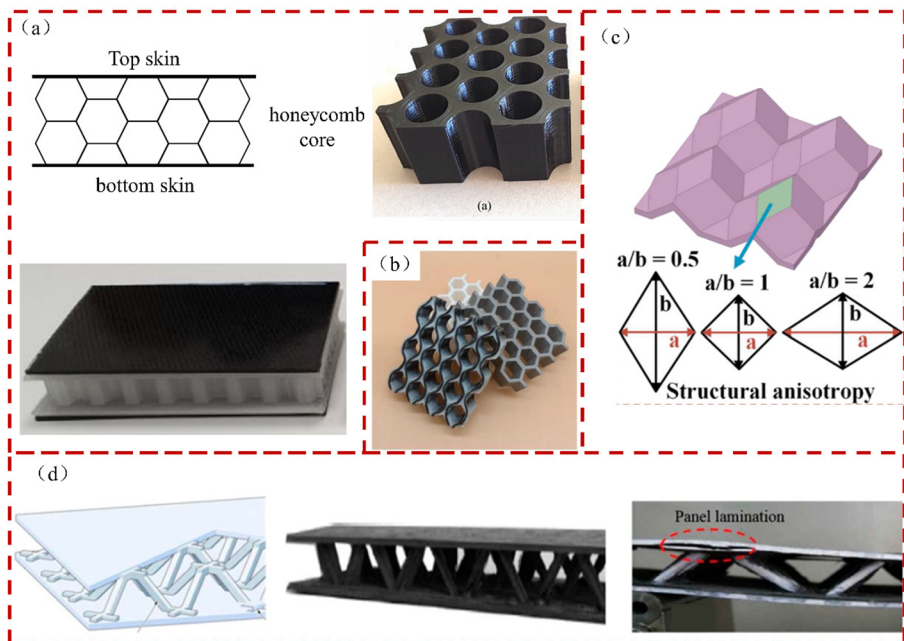


**Fig. 29** Additive manufacturing of CFRCs honeycomb structures: **a** Honeycomb board structure schematic [140, 141]; **b** Honeycomb panel sandwich prepared by CCFRC [142] **c** and **d** Sandwich panels with three-dimensional sandwich structure [143, 144]

Kang et al. [148], which can not only realize thermal deformation in different temperature environments, but can also be used to regulate the transmission properties of electromagnetic waves. In addition, CFRCs have unique advantages in the field of acoustics, taking advantage of their multifaceted characteristics to achieve excellent sound absorption and vibration isolation properties [149]. As shown in Fig. 30c, a carbon fiber honeycomb was incorporated as a backbone into the acoustic periodic array structure, achieving an absorption bandwidth of 0.9 at 2400–10000 Hz and 1.5 MPa hydraulic pressure [150]. With the rise of AM, more and more acoustic structures will be designed and realized.

## 6 Challenges and Problems

This paper describes the current feasible methods for AM of CFRCs and highlights the current status of research on the preparation of CFRC parts by FDM and SLS. Compared to traditional manufacturing, AM has tremendous potential to reduce time to market, provide personalized service, and expand design options. However, the manufacturing accuracy

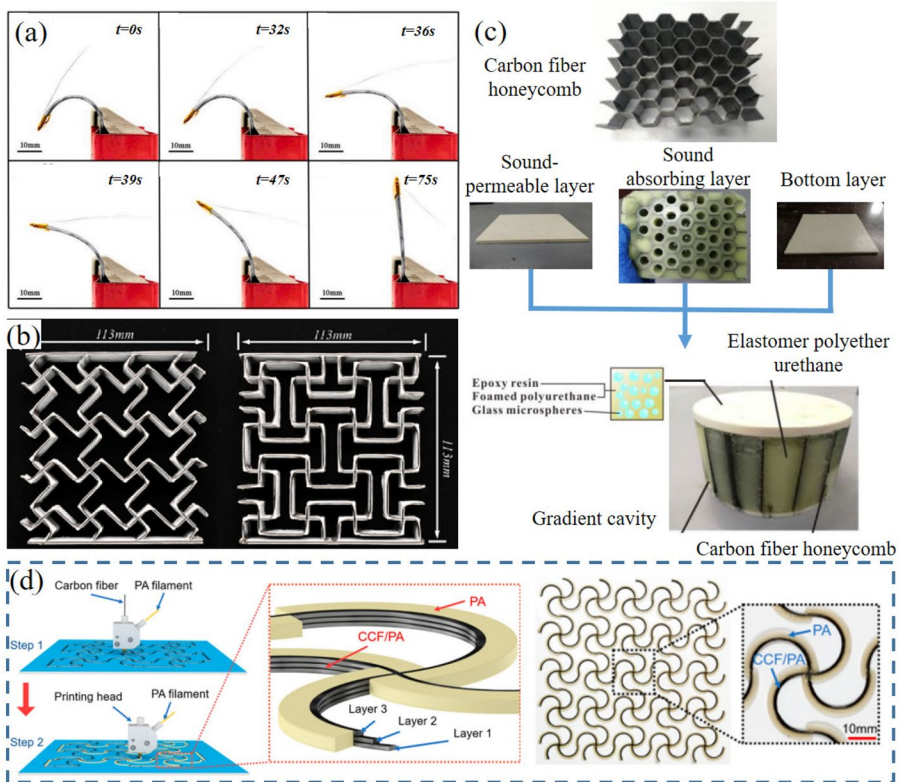


**Fig. 30** 4D printing of CFRCs: **a** Snapshot of Joule heating-induced shape recovery in 4D printed CCFRCs [146]; **b** The auxiliary auxetic structure was innovatively printed using a continuous-fiber-reinforced polydimethylsiloxane composite [149]; **c** Fabrication procedures of carbon fiber honeycomb supported sound-absorbing periodically arrayed structure [150]; **d** Strategies for 4D printing continuous carbon fiber-reinforced PA hypersurface structures [148]

**Table 2** Cite article classification

Process	Fiber	Matrix	Content of the study
FDM	CCF	ABS [15, 45, 75, 89], PA [36, 38, 72, 98, 102, 103, 121], PLA [6, 35, 40, 46, 85, 86, 109, 153], Polycarbonate [113], Polypropylene [97], Portland cement paste [69], Epoxy resin [47–49], PEEK [16, 111], TPI [44], Onyx [71]	Mechanical property
		PLA [17, 79, 99, 151], PA [37, 80, 87], ABS [34, 90], PEEK [88]	Molding process
		PLA [96, 115], PA [39, 116, 118], PETG [114]	Failure mode
		PLA [140, 142], PA [76, 117, 148], SR [135], PLA [132, 138, 145–147], PTMS [149], Epoxy resin [137], PDMS [149], PA [148]	Structural design
	SCF	PEEK[14], ABS [82, 94], PLA [73, 100, 105, 106], Geopolymer [2, 93], PP [70], Thermoset matrix [112], PBT [56], PA [41, 84], Epoxy resin [91], Polyene resin [92], PET [29]	Applications
		PA6 [81, 83, 123], PEEK [13], PLA [74, 77]	Mechanical property
		ABS [101], Nylon [143]	Molding process
		PEEK [134]	Structural design
SLS	SCF	PA12 [30, 50, 59, 119, 122, 126, 127], Si [58], Wollastonite [55], PAN [31]	Applications
		PEKK [110], PEEK [53], PA12 [123]	Mechanical property
		PA12 [54, 57]	Molding process
Lc-AM	SCF	photosensitive resin [61]	Failure mode
Ra-AM	CCF	PEE [7]	Molding process
GM	CCF	PLA [65–67], Diglycidyl bisphenol-A [64], PETG [63]	Mechanical property
Other Processes	CCF	TPI [42]	Mechanical property
		Polyurethane [150]	Mechanical property
	SCF	PA6 [120]	Applications
		PEEK [129, 130],	Structural design
Other Articles	Nanomaterials	GO [22, 23, 25, 26, 28], CNTs [24, 27], I-MBP-PCF [21]	Applications
			Surface modification

and flexibility of additive manufactured CFRCs are also limited by raw materials, equipment, and path-planning algorithms.

For the raw materials, carbon fiber prepregs with excellent initial properties should be selected to facilitate subsequent additive manufacturing. As described in this paper, the preparation technique of short carbon fiber prepreg is simpler than that of continuous carbon fiber prepreg, but the mechanical properties of the fabricated parts are much less outstanding than those of continuous carbon fiber parts. High-performance continuous carbon fiber prepregs should have low porosity, a high degree of resin encapsulation, and uniform carbon fiber dispersion. So far, the carbon fiber prepregs reported in the literature are judged by tensile strength and modulus, while there is no unified standard to quantify the properties of porosity, resin encapsulation, and carbon fiber dispersion.

For the equipment, the current gantry system limits the part size and complexity. Moreover, the free deposition method is difficult to form dense parts. Therefore, robot-assisted additive manufacturing technology has received more attention. The multiple degrees of freedom robot system allows changing the accumulation direction during the additive manufacturing process, making it feasible for printing curve and overhang features without support. However, some critical issues need to be addressed in robot-assisted additive manufacturing. First of all, the mainstream slicing software on the market cannot generate G-code data compatible with the robot language, making it difficult to quickly obtain multi-model slicing data adapted to the robot language. Furthermore, robot-assisted additive manufacturing has low precision, which may affect the subsequent processing and mechanical properties of the part. Finally, for the fabrication of some large objects, multiple robots need to be used simultaneously, but this poses a synergy problem.

For the planning algorithm, there have been many studies on continuous path algorithms for honeycomb structures, but these algorithms are not suitable for all targets. In the process of additive manufacturing, large corners and intersections in the print path need to be avoided to control part accuracy, but these factors have not been fully considered [151]. In addition, for heterogeneous objects, how to macroscopically set the start point of each layer path is also a key factor for the path planning, while this has not been reported yet. Therefore, path planning remains one of the key issues for continuous carbon fiber additive manufacturing. A set of path-planning algorithms that can be used for a variety of complex structures urgently needs to be developed to make continuous carbon fiber additive manufacturing more flexible.

## 7 Outlook

This paper reviews the raw materials, processes, and equipment related to additive manufacturing of carbon fiber reinforced composites and all the literature is detailed in Table 2. After the above summary, the future direction of additive manufacturing CFRC can be obtained:

1. High-quality and high-volume content carbon fiber prepreg is the development direction of fiber prepreg. The raw material' goodness directly affects the performance of the formed component. Different CFRC additive technologies have different requirements for raw materials. Carbon fiber prepreg tape process and equipment are mature, but ATP, FDM, and other processes of carbon fiber prepreg material is not yet fully commercialized. Moreover, the current carbon fiber prepreg filaments have a relatively

- high porosity, fiber content is low, low porosity (less than 1%), high specific content (more than 50%) of high-quality carbon fiber prepreg is urgently needed.
2. The optimization of process parameters is still the focus of research in the future. Any CCFRC part with high mechanical properties cannot be achieved without an optimal combination of process parameters, which should also cover the planning of fiber paths. Exploring the effects of force, temperature, and fiber path on the CCFRC additive molding process will help us better control the parts' properties.
  3. Exploring the process mechanism through the simulation method is the development direction of the process research of additively manufactured carbon fiber reinforced composites. The processing core is the resin melting and solidification forming process in the composite filament, and the related process research focuses on single-factor or multi-factor experimental research. However, some of the additive process is exceptionally complex, such as ATP, robotic additive manufacturing, and other processes. Under the action of laser radiation, the resin is melted and solidified. In this process, there are energy absorption, conversion, and transfer, as well as the effect of resin melting flow field and external pressure. Therefore, it is very difficult to model this process, and the key is to construct a multi-field coupled heat-force-flow model.
  4. Additive manufacturing CFRCs can be used in structural lightweight design and functional empowerment. For the former, a wider variety of honeycomb porous structures can be developed. For example, the standard hexagonal honeycomb has evolved from the basic cell shape to variations of truncated-square, reentrant hexangular core, and chiral honeycombs which facilitates the combination of both mechanical and thermal properties for efficient structural load support and thermal management [139, 152]. The lattice structure is expected to further reduce the weight of carbon fiber components while achieving customizable mechanical properties. For the latter, additively manufactured parts can be given more functionality, such as acoustic, thermal, and shape memory properties, i.e., expanding from 3D printing to 4D printing.
  5. Additive manufacturing of CFRCs is moving towards a multi-material/gradient design. Currently, most additive manufacturing equipment can only form single material components with relatively uniform internal material distribution. However, due to the obvious directionality of continuous carbon fiber properties, different filling strategies, different filling densities or different filling materials can be obtained through path planning, to achieve different properties. Therefore, the manufacturing of carbon fiber reinforced composite components with multi-material/gradient design through the additive manufacturing will be an important direction in the future.

In summary, carbon fiber additive manufacturing is still in its initial stage, many structures have not been realized yet, and more functions have not been explored yet. To achieve these goals, it will be a great challenge to integrate advanced materials, smart devices, precise processes, clever structural designs, and other fields.

**Funding** The study was supported by the Key Research and Development Plan of Hubei Province (2022BAA030 and 2021BAA211) and the National Natural Science Foundation of China (No. 52235008).

**Author Contribution** Yong Hu: Investigation, Formal analysis, Software. Yudong Lin: Data curation, Visualizations, Writing - Original Draft. Lei Yang: Conceptualization, Methodology, Writing - Review & Editing, Funding acquisition. Siqi Wu: Writing - Review & Editing. DianYu Tang: Writing - Review & Editing. Chunze Yan: Writing - Review & Editing. Yusheng Shi: Writing - Review & Editing.

**Availability of Data and Material** Data sharing not applicable to this article as no datasets were generated or analyzed during the current study.

## Declarations

**Competing of Interest** The authors declare that they have no known competing financial interests or personal relationships that could have appeared to influence the work reported in this paper.

## References

1. Muna, II., Mieloszyk, M.: Temperature Influence on Additive Manufactured Carbon Fiber Reinforced Polymer Composites. *Materials (Basel)* **14**(21), 6413 (2021). <https://doi.org/10.3390/ma14216413>
2. Korniejenko, K., Lach, M., Chou, S.Y., et al.: Mechanical Properties of Short Fiber-Reinforced Geopolymers Made by Casted and 3D Printing Methods: A Comparative Study. *Materials (Basel)* **13**(3), 579 (2020). <https://doi.org/10.3390/ma13030579>
3. Yang, L., Wu, S., Yan, C., et al.: Fatigue properties of Ti-6Al-4V Gyroid graded lattice structures fabricated by laser powder bed fusion with lateral loading. *Addit. Manuf.* **46**, (2021). <https://doi.org/10.1016/j.addma.2021.102214>
4. Zhang, C., Zheng, H., Yang, L., et al.: Mechanical responses of sheet-based gyroid-type triply periodic minimal surface lattice structures fabricated using selective laser melting. *Mater. Des.* **214**, (2022). <https://doi.org/10.1016/j.matdes.2022.110407>
5. van de Werken, N., Tekinalp, H., Khanbolouki, P., et al.: Additively manufactured carbon fiber-reinforced composites: State of the art and perspective. *Addit. Manuf.* **31**, 100962 (2020). <https://doi.org/10.1016/j.addma.2019.100962>
6. Zhang, Z., Long, Y., Yang, Z., et al.: An investigation into printing pressure of 3D printed continuous carbon fiber reinforced composites. *Compos. A Appl. Sci. Manuf.* **162**, 107162 (2022). <https://doi.org/10.1016/j.compositesa.2022.107162>
7. Clancy, G., Peeters, D., Oliveri, V., et al.: A study of the influence of processing parameters on steering of carbon Fibre/PEEK tapes using laser-assisted tape placement. *Compos. B Eng.* **163**, 243–251 (2019). <https://doi.org/10.1016/j.compositesb.2018.11.033>
8. Prüß, H., Vietor, T.: Design for Fiber-Reinforced Additive Manufacturing. *J. Mech. Des.* **137**(11), (2015). <https://doi.org/10.1115/1.4030993>
9. Dikshit, V., Goh, G.D., Nagalingam, A.P., et al.: Recent progress in 3D printing of fiber-reinforced composite and nanocomposites. *Fiber-Reinforced Nanocomposites: Fundam. Appl.* 371–94 (2020). <https://doi.org/10.1016/b978-0-12-819904-6.00017-7>
10. Pervaiz, S., Qureshi, T.A., Kashwani, G., et al.: 3D Printing of Fiber-Reinforced Plastic Composites Using Fused Deposition Modeling: A Status Review. *Materials (Basel)* **14**(16), 4520 (2021). <https://doi.org/10.3390/ma14164520>
11. Adil S, Lazoglu I. A review on additive manufacturing of carbon fiber-reinforced polymers: Current methods, materials, mechanical properties, applications and challenges. *Journal of Applied Polymer Science*, 140(7). (2022) <https://doi.org/10.1002/app.53476>
12. Tian, X., Todoroki, A., Liu, T., et al.: 3D Printing of Continuous Fiber Reinforced Polymer Composites: Development, Application, and Prospective. *Chinese Journal of Mechanical Engineering: Additive Manufacturing Frontiers* **1**(1), 100016 (2022). <https://doi.org/10.1016/j.cjmeam.2022.100016>
13. Yang, D., Cao, Y., Zhang, Z., et al.: Effects of crystallinity control on mechanical properties of 3D-printed short-carbon-fiber-reinforced polyether ether ketone composites. *Polym. Testing* **97**, 107149 (2021). <https://doi.org/10.1016/j.polymertesting.2021.107149>
14. Wang, P., Zou, B., Ding, S., et al.: Preparation of short CF/GF reinforced PEEK composite filaments and their comprehensive properties evaluation for FDM-3D printing. *Compos. B Eng.* **198**, 108175 (2020). <https://doi.org/10.1016/j.compositesb.2020.108175>
15. Rimašauskas, M., Kuncius, T., Rimašauskienė, R.: Processing of carbon fiber for 3D printed continuous composite structures. *Mater. Manuf. Processes* **34**(13), 1528–1536 (2019). <https://doi.org/10.1080/10426914.2019.1655152>
16. Barış, Vatandaş, B., Uşun, A., Yıldız, N., et al. Additive manufacturing of PEEK-based continuous fiber reinforced thermoplastic composites with high mechanical properties. *Composites Part A: Appl. Mater. Sci.* **158**, 106753 (2023). <https://doi.org/10.1016/j.compositesa.2023.106753>

- Appl. Sci. Manuf. **167**(April 2023), 107434 (2023). <https://doi.org/10.1016/j.compositesa.2023.107434>
17. Uşun, A., GüMRüK, R.: The mechanical performance of the 3D printed composites produced with continuous carbon fiber reinforced filaments obtained via melt impregnation. *Addit. Manuf.* **46**, 102112 (2021). <https://doi.org/10.1016/j.addma.2021.102112>
  18. Qiao, J., Li, Y., Li, L.: Ultrasound-assisted 3D printing of continuous fiber-reinforced thermoplastic (FRTP) composites. *Addit. Manuf.* **30**, 100926 (2019). <https://doi.org/10.1016/j.addma.2019.100926>
  19. Hu, Q., Duan, Y., Zhang, H., et al.: Manufacturing and 3D printing of continuous carbon fiber prepreg filament. *J. Mater. Sci.* **53**(3), 1887–1898 (2017). <https://doi.org/10.1007/s10853-017-1624-2>
  20. Cano-Vicent, A., Tambuwala, M.M., Hassan, S.S., et al.: Fused deposition modelling: Current status, methodology, applications and future prospects. *Addit. Manuf.* **47**, 102378 (2021). <https://doi.org/10.1016/j.addma.2021.102378>
  21. Wu, Y., Cheng, X., Chen, S., et al.: In situ formation of a carbon nanotube buckypaper for improving the interlaminar properties of carbon fiber composites. *Mater. Des.* **202**, (2021). <https://doi.org/10.1016/j.matdes.2021.109535>
  22. Qiu, B., Sun, T., Yuan, M., et al.: Effect of different lateral dimension graphene oxide sheets on the interface of carbon fiber reinforced polymer composites. *Compos. Sci. Technol.* **213**, (2021). <https://doi.org/10.1016/j.compscitech.2021.108939>
  23. Sun, T., Li, M., Zhou, S., et al.: Multi-scale structure construction of carbon fiber surface by electrophoretic deposition and electropolymerization to enhance the interfacial strength of epoxy resin composites. *Appl. Surf. Sci.* **499**, (2020). <https://doi.org/10.1016/j.apsusc.2019.143929>
  24. Gao, B., Zhang, R., He, M., et al.: Effect of a multiscale reinforcement by carbon fiber surface treatment with graphene oxide/carbon nanotubes on the mechanical properties of reinforced carbon/carbon composites. *Compos. A Appl. Sci. Manuf.* **90**, 433–440 (2016). <https://doi.org/10.1016/j.compositesa.2016.08.012>
  25. Jiang, J., Yao, X., Xu, C., et al.: Preparation of Graphene Oxide Coatings onto Carbon Fibers by Electrophoretic Deposition for Enhancing Interfacial Strength in Carbon Fiber Composites. *J. Electrochem. Soc.* **163**(5), D133–D139 (2016). <https://doi.org/10.1149/2.0571605jes>
  26. Deng, C., Jiang, J., Liu, F., et al.: Influence of graphene oxide coatings on carbon fiber by ultrasonically assisted electrophoretic deposition on its composite interfacial property. *Surf. Coat. Technol.* **272**, 176–181 (2015). <https://doi.org/10.1016/j.surfcoat.2015.04.008>
  27. Lee, S-B, Choi, O., Lee, W., et al.: Processing and characterization of multi-scale hybrid composites reinforced with nanoscale carbon reinforcements and carbon fibers. *Composites Part A: Appl. Sci. Manuf.* **42**(4), 337–44 (2011). <https://doi.org/10.1016/j.compositesa.2010.10.016>
  28. Fu, J., Zhang, M., Jin, L., et al.: Enhancing interfacial properties of carbon fibers reinforced epoxy composites via Layer-by-Layer self assembly GO/SiO<sub>2</sub> multilayers films on carbon fibers surface. *Appl. Surf. Sci.* **470**, 543–554 (2019). <https://doi.org/10.1016/j.apsusc.2018.11.168>
  29. Shi, P., Wu, W., Chen, Y., et al.: Influence of Fiber Surface Treatment on Mechanical Properties of CF/PET Composites. *J. Macromol. Sci. Phys. Part B* **51**(8), 1485–1497 (2011). <https://doi.org/10.1080/00222348.2011.632740>
  30. Yan, C., Hao, L., Xu, L., et al.: Preparation, characterisation and processing of carbon fibre/polyamide-12 composites for selective laser sintering. *Compos. Sci. Technol.* **71**(16), 1834–1841 (2011). <https://doi.org/10.1016/j.compscitech.2011.08.013>
  31. Yan, Q-S., Wei, R., Lu, G., et al.: Effect of modified carbon fibres on the performance of the coated sand by selected laser sintering. *Mater. Res. Inn.* **19**, S6–54-S6–8 (2015). <https://doi.org/10.1179/1432891715z.0000000001446>
  32. Jing, W., Hui, C., Qiong, W., et al.: Surface modification of carbon fibers and the selective laser sintering of modified carbon fiber/nylon 12 composite powder. *Mater. Des.* **116**, 253–260 (2017). <https://doi.org/10.1016/j.matdes.2016.12.037>
  33. Dixit, N., Jain, P.K.: 3D printed carbon fiber reinforced thermoplastic composites: A review. *Mater. Today Proc.* **43**, 678–681 (2021). <https://doi.org/10.1016/j.matpr.2020.12.609>
  34. Prusinowski, A., Kaczyński, R.: Investigation of Tribological and Strength Properties of ABS/CF Fibrous Composites Formed in Fused Deposition Modeling. *J. Frict. Wear.* **41**(4), 318–325 (2020). <https://doi.org/10.3103/s106836662004011x>
  35. Luo, H., Tan, Y., Zhang, F., et al.: Selectively Enhanced 3D Printing Process and Performance Analysis of Continuous Carbon Fiber Composite Material. *Materials (Basel)* **12**(21), 3529 (2019). <https://doi.org/10.3390/ma12213529>



36. Iragi, M., Pascual-González, C., Esnaol, A.A., et al.: Ply and interlaminar behaviours of 3D printed continuous carbon fibre-reinforced thermoplastic laminates; effects of processing conditions and microstructure. *Addit. Manuf.* **30**, 100884 (2019). <https://doi.org/10.1016/j.addma.2019.100884>
37. Zhang, H., Chen, J., Yang, D.: Fibre misalignment and breakage in 3D printing of continuous carbon fibre reinforced thermoplastic composites. *Addit. Manuf.* **38**, 101775 (2021). <https://doi.org/10.1016/j.addma.2020.101775>
38. Chacón, J.M., Caminero, M.Á., Núñez, P.J., et al.: Effect of nozzle diameter on mechanical and geometric performance of 3D printed carbon fibre-reinforced composites manufactured by fused filament fabrication. *Rapid Prototyp. J.* **27**(4), 769–84 (2021). <https://doi.org/10.1108/rpj-10-2020-0250>
39. Justo, J., Távora, L., García-Guzmán, L., et al.: Characterization of 3D printed long fibre reinforced composites. *Compos. Struct.* **185**, 537–48 (2018). <https://doi.org/10.1016/j.compstruct.2017.11.052>
40. Matsuzaki, R., Ueda, M., Namiki, M., et al.: Three-dimensional printing of continuous-fiber composites by in-nozzle impregnation. *Sci. Rep.* **6**, 23058 (2016). <https://doi.org/10.1038/srep23058>
41. Peng, Y., Wu, Y., Wang, K., et al.: Synergistic reinforcement of polyamide-based composites by combination of short and continuous carbon fibers via fused filament fabrication. *Compos. Struct.* **207**, 232–239 (2019). <https://doi.org/10.1016/j.compstruct.2018.09.014>
42. Nam, T.H., Goto, K., Kamei, T., et al.: Improved mechanical properties of aligned multi-walled carbon nanotube/thermoplastic polyimide composites by hot stretching. *J. Compos. Mater.* **53**(9), 1241–1253 (2018). <https://doi.org/10.1177/0021998318796916>
43. Wu, W., Ye, W., Geng, P., et al.: 3D printing of thermoplastic PI and interlayer bonding evaluation. *Mater. Lett.* **229**, 206–209 (2018). <https://doi.org/10.1016/j.matlet.2018.07.020>
44. Ye, W., Lin, G., Wu, W., et al.: Separated 3D printing of continuous carbon fiber reinforced thermoplastic polyimide. *Compos. A Appl. Sci. Manuf.* **121**, 457–464 (2019). <https://doi.org/10.1016/j.compositesa.2019.04.002>
45. Yang, C., Tian, X., Liu, T., et al.: 3D printing for continuous fiber reinforced thermoplastic composites: mechanism and performance. *Rapid Prototyp. J.* **23**(1), 209–215 (2017). <https://doi.org/10.1108/rpj-08-2015-0098>
46. Tian, X., Liu, T., Yang, C., et al.: Interface and performance of 3D printed continuous carbon fiber reinforced PLA composites. *Compos. A Appl. Sci. Manuf.* **88**, 198–205 (2016). <https://doi.org/10.1016/j.compositesa.2016.05.032>
47. Ming, Y., Duan, Y., Wang, B., et al.: A Novel Route to Fabricate High-Performance 3D Printed Continuous Fiber-Reinforced Thermosetting Polymer Composites. *Materials (Basel)* **12**(9), 1369 (2019). <https://doi.org/10.3390/ma12091369>
48. Rahman, M.A., Islam, M.Z., Gibbon, L., et al.: 3D printing of continuous carbon fiber reinforced thermoset composites using UV curable resin. *Polym. Compos.* **42**(11), 5859–5868 (2021). <https://doi.org/10.1002/pc.26266>
49. Hao, W., Liu, Y., Zhou, H., et al.: Preparation and characterization of 3D printed continuous carbon fiber reinforced thermosetting composites. *Polym. Testing* **65**, 29–34 (2018). <https://doi.org/10.1016/j.polymertesting.2017.11.004>
50. Floersheim, R.B., Hou, G., Firestone, K.: CFPC material characteristics and SLS prototyping process. *Rapid Prototyp. J.* **15**(5), 339–345 (2009). <https://doi.org/10.1108/13552540910993860>
51. Gu, D.D., Meiners, W., Wissenbach, K., et al.: Laser additive manufacturing of metallic components: materials, processes and mechanisms. *Int. Mater. Rev.* **57**(3), 133–164 (2013). <https://doi.org/10.1179/1743280411y.0000000014>
52. Singh, S., Sharma, V.S., Sachdeva, A.: Optimization and Analysis of Shrinkage in Selective Laser Sintered Polyamide Parts. *Mater. Manuf. Processes* **27**(6), 707–714 (2012). <https://doi.org/10.1080/10426914.2011.593247>
53. Yan, M., Tian, X., Peng, G., et al.: High temperature rheological behavior and sintering kinetics of CF/PEEK composites during selective laser sintering. *Compos. Sci. Technol.* **165**, 140–147 (2018). <https://doi.org/10.1016/j.compscitech.2018.06.023>
54. Effect of reinforcement and temperature: Salazar A, Rico A, RODRÍGUEZ J, et al. Fatigue crack growth of SLS polyamide 12. *Compos. B Eng.* **59**, 285–292 (2014). <https://doi.org/10.1016/j.compositesb.2013.12.017>
55. Kleijnen, R.G., Sesseg, J.P.W., Schmid, M., et al.: Insights into the development of a short-fiber reinforced polypropylene for laser sintering; proceedings of the AIP Conference Proceedings, F, (2017). AIP Publishing LLC.

56. Arai, S., Tsunoda, S., Yamaguchi, A., et al.: Effects of short-glass-fiber content on material and part properties of poly(butylene terephthalate) processed by selective laser sintering. *Addit. Manuf.* **21**, 683–693 (2018). <https://doi.org/10.1016/j.addma.2018.04.019>
57. Liu, Y., Zhu, L., Zhou, L., et al.: Microstructure and mechanical properties of reinforced polyamide 12 composites prepared by laser additive manufacturing. *Rapid Prototyping Journal* **25**(6), 1127–1134 (2019). <https://doi.org/10.1108/rpjm-08-2018-0220>
58. Zou, Y., Li, C-H., Hu, L., et al.: Effects of short carbon fiber on the macro-properties, mechanical performance and microstructure of SiSiC composite fabricated by selective laser sintering. *Ceram. Int.* **46**(8), 12102–10 (2020). <https://doi.org/10.1016/j.ceramint.2020.01.255>
59. Zhu, W., Yan, C., Shi, Y., et al.: A novel method based on selective laser sintering for preparing high-performance carbon fibres/polyamide12/epoxy ternary composites. *Sci. Rep.* **6**, 33780 (2016). <https://doi.org/10.1038/srep33780>
60. Pagac, M., Hajnys, J., Ma, Q.P., et al.: A Review of Vat Photopolymerization Technology: Materials, Applications, Challenges, and Future Trends of 3D Printing. *Polymers (Basel)* **13**(4), 598 (2021). <https://doi.org/10.3390/polym13040598>
61. Asif, S., Chansoria, P., Shirwaiker, R.: Ultrasound-assisted vat photopolymerization 3D printing of preferentially organized carbon fiber reinforced polymer composites. *J. Manuf. Process.* **56**, 1340–1343 (2020). <https://doi.org/10.1016/j.jmappro.2020.04.029>
62. Arevo Applications. <https://arevo.com/applications>. Accessed 26 June 2019
63. Romani, A., Caba, S., Suriano, R., et al.: Recycling Glass and Carbon Fibers for Reusable Components in the Automotive Sector through Additive Manufacturing. *Appl. Sci.* **13**(10), (2023). <https://doi.org/10.3390/app13105848>
64. Jeong, J.S., Kim, K.W., An, K.H., et al.: Fast recovery process of carbon fibers from waste carbon fibers-reinforced thermoset plastics. *J. Environ. Manage.* **247**, 816–821 (2019). <https://doi.org/10.1016/j.jenvman.2019.07.002>
65. Tian, X., Liu, T., Wang, Q., et al.: Recycling and remanufacturing of 3D printed continuous carbon fiber reinforced PLA composites. *J. Clean. Prod.* **142**, 1609–1618 (2017). <https://doi.org/10.1016/j.jclepro.2016.11.139>
66. Cheng, H., Guo, L., Qian, Z., et al.: Remanufacturing of recycled carbon fiber-reinforced composites based on fused deposition modeling processes. *Int. J. Adv. Manuf. Technol.* **116**(5–6), 1609–1619 (2021). <https://doi.org/10.1007/s00170-021-07473-w>
67. Huang, H., Liu, W., Liu, Z.: Additive manufacturing-inspired approach to re-manufacture fiber reinforced plastic with programmable orientation of recycled carbon fiber. *Compos. Commun.* **38**, (2023). <https://doi.org/10.1016/j.coco.2023.101521>
68. Romanowski, H., Bierkandt, F.S., Luch, A., et al.: Summary and derived Risk Assessment of 3D printing emission studies. *Atmos. Environ.* **294**, (2023). <https://doi.org/10.1016/j.atmosenv.2022.119501>
69. Hambach, M., Volkmer, D.: Properties of 3D-printed fiber-reinforced Portland cement paste. *Cement Concr. Compos.* **79**, 62–70 (2017). <https://doi.org/10.1016/j.cemconcomp.2017.02.001>
70. Spoerk, M., Savandiah, C., Arbeiter, F., et al.: Anisotropic properties of oriented short carbon fibre filled polypropylene parts fabricated by extrusion-based additive manufacturing. *Compos. A Appl. Sci. Manuf.* **113**, 95–104 (2018). <https://doi.org/10.1016/j.compositesa.2018.06.018>
71. Silvestri, A.T., Papa, I., Squillace, A.: Influence of Fibre Fill Pattern and Stacking Sequence on Open-Hole Tensile Behaviour in Additive Manufactured Fibre-Reinforced Composites. *Materials (Basel)* **16**(6), (2023). <https://doi.org/10.3390/ma16062411>
72. Mishra, P.K., Jagadesh, T.: Investigations into flexural behavior of additively manufactured short and continuous fiber CFRP composites. *J. Braz. Soc. Mech. Sci. Eng.* **45**(3), (2023). <https://doi.org/10.1007/s40430-023-04085-1>
73. Yan, J., Demirci, E., Gleadal, A.: 3D short fibre orientation for universal structures and geometries in material extrusion additive manufacturing. *Addit. Manuf.* **69**, (2023). <https://doi.org/10.1016/j.addma.2023.103535>
74. Lian, K., Yang, L., Zhu, D., et al.: Effect of printing parameters on 3D-printed carbon fiber-reinforced polymer composites under magnetic field control. *J. Manuf. Process.* **101**, 1443–1452 (2023). <https://doi.org/10.1016/j.jmappro.2023.07.040>
75. Nakagawa, Y., Mori, K-I., Maeno, T.: 3D printing of carbon fibre-reinforced plastic parts. *Int. J. Adv. Manuf. Technol.* **91**(5–8), 2811–7 (2017). <https://doi.org/10.1007/s00170-016-9891-7>
76. Li, N., Link, G., Wang, T., et al.: Path-designed 3D printing for topological optimized continuous carbon fibre reinforced composite structures. *Compos. B Eng.* **182**, 31245–31254 (2020). <https://doi.org/10.1016/j.compositesb.2019.107612>

77. Kipping, J., Schuppstuh, L.T.: Load-Oriented Nonplanar Additive Manufacturing Method for Optimized Continuous Carbon Fiber Parts. *Materials (Basel)* **16**(3), (2023). <https://doi.org/10.3390/ma16030998>
78. Huang, Y., Fang, G., Zhang, T., et al.: Turning-angle optimized printing path of continuous carbon fiber for cellular structures. *Addit. Manuf.* **68**, (2023). <https://doi.org/10.1016/j.addma.2023.103501>
79. Tu, Y., Tan, Y., Zhang, F., et al.: Shearing algorithm and device for the continuous carbon fiber 3D printing. *J. Adv. Mech. Des. Syst. Manuf.* **13**(1), JAMDSM0016-JAMDSM. (2019). <https://doi.org/10.1299/jamdsm.2019jamdsm0016>
80. Abas, M., Awadh, M.A., Habib, T., et al.: Analyzing Surface Roughness Variations in Material Extrusion Additive Manufacturing of Nylon Carbon Fiber Composites. *Polymers (Basel)* **15**(17), (2023). <https://doi.org/10.3390/polym15173633>
81. Barera, G., Dul, S., Pegoretti, A.: Screw Extrusion Additive Manufacturing of Carbon Fiber Reinforced PA6 Tools. *J. Mater. Eng. Perform.* (2023). <https://doi.org/10.1007/s11665-023-08238-0>
82. Yan, J., Demirci, E., Ganesan, A., et al.: Extrusion width critically affects fibre orientation in short fibre reinforced material extrusion additive manufacturing. *Addit. Manuf.* **49**, 102496 (2022). <https://doi.org/10.1016/j.addma.2021.102496>
83. Benfriha, K., Ahmadifar, M., Shirinbayan, M., et al.: Effect of process parameters on thermal and mechanical properties of polymer-based composites using fused filament fabrication. *Polym. Compos.* **42**(11), 6025–6037 (2021). <https://doi.org/10.1002/pc.26282>
84. Tutar, M.A.: Comparative Evaluation of the Effects of Manufacturing Parameters on Mechanical Properties of Additively Manufactured PA and CF-Reinforced PA Materials. *Polymers (Basel)*, **15**(1), (2022). <https://doi.org/10.3390/polym15010038>
85. Dou, H., Cheng, Y., Ye, W., et al.: Effect of Process Parameters on Tensile Mechanical Properties of 3D Printing Continuous Carbon Fiber-Reinforced PLA Composites. *Materials (Basel)* **13**(17), 3850 (2020). <https://doi.org/10.3390/ma13173850>
86. Jia, Z., Wang, Q., Liu, J.: An Investigation of Printing Parameters of Independent Extrusion Type 3D Print Continuous Carbon Fiber-Reinforced PLA. *Appl. Sci.* **13**(7), (2023). <https://doi.org/10.3390/app13074222>
87. Chen, Z., Zhang, Z., Granland, K., et al.: Exploring optimal adaptive process parameters for curved infill paths of additive manufactured carbon fibre reinforced polymers. *Compos. Commun.* **39**, (2023). <https://doi.org/10.1016/j.coco.2023.101549>
88. Ji, Y., Luan, C., Yao, X., et al.: Mechanism and behavior of laser irradiation on carbon fiber reinforced polyetheretherketone (CF/PEEK) during the laser-assisted in-situ consolidation additive manufacturing process. *Addit. Manuf.* **74**, (2023). <https://doi.org/10.1016/j.addma.2023.103713>
89. Tekinalp, H.L., Kunc, V., Velez-Garcia, G.M., et al.: Highly oriented carbon fiber–polymer composites via additive manufacturing. *Compos. Sci. Technol.* **105**, 144–150 (2014). <https://doi.org/10.1016/j.compscitech.2014.10.009>
90. Blok, L.G., Longana, M.L., Yu, H., et al.: An investigation into 3D printing of fibre reinforced thermoplastic composites. *Addit. Manuf.* **22**, 176–186 (2018). <https://doi.org/10.1016/j.addma.2018.04.039>
91. Melenka, G.W., Cheung, B.K.O., Schofield, J.S., et al.: Evaluation and prediction of the tensile properties of continuous fiber-reinforced 3D printed structures. *Compos. Struct.* **153**, 866–875 (2016). <https://doi.org/10.1016/j.compstruct.2016.07.018>
92. Sheng, Y.H.: Different Content of Short Carbon Fiber Influence on the Hardness of Thermo Plastic Resin Composite Material. *Appl. Mech. Mater.* **490–491**, 280–283 (2014). <https://doi.org/10.4028/www.scientific.net/AMM.490-491.280>
93. Lin, T., Jia, D., Wang M., et al.: Effects of fibre content on mechanical properties and fracture behaviour of short carbon fibre reinforced geopolymer matrix composites. *Bull. Mater. Sci.* **32**(1), 77–81 (2009). <https://doi.org/10.1007/s12034-009-0011-2>
94. Somireddy, M., Singh, C.V., Czekanski, A.: Mechanical behaviour of 3D printed composite parts with short carbon fiber reinforcements. *Eng. Fail. Anal.* **107**, 104232 (2020). <https://doi.org/10.1016/j.engfailanal.2019.104232>
95. Yang, D., Zhang, H., Wu, J., et al.: Fibre flow and void formation in 3D printing of short-fibre reinforced thermoplastic composites: An experimental benchmark exercise. *Addit. Manuf.* **37**, 101686 (2021). <https://doi.org/10.1016/j.addma.2020.101686>
96. Papon, E.A., Haque, A.: Fracture toughness of additively manufactured carbon fiber reinforced composites. *Addit. Manuf.* **26**, 41–52 (2019). <https://doi.org/10.1016/j.addma.2018.12.010>
97. Fu, S., Lauke, B., Mader, E., et al.: Tensile properties of short-glass-fiber- and short-carbon-fiber-reinforced polypropylene composites. *Compos. A Appl. Sci. Manuf.* **31**(10), 1117–1125 (2000)

98. He, Q., Wang, H., Fu, K., et al.: 3D printed continuous CF/PA6 composites: Effect of microscopic voids on mechanical performance. *Compos. Sci. Technol.* **191**, 108077 (2020). <https://doi.org/10.1016/j.compscitech.2020.108077>
99. Li, H., Lou, R., Liu, B., et al.: Research on the fusion of continuous fiber reinforced thermoplastic filaments for fused filament fabrication. *Int. J. Solids Struct.* **276**, (2023). <https://doi.org/10.1016/j.ijsolstr.2023.112328>
100. Pappas, J.M., Thakur, A.R., Leu, M.C., et al.: A Comparative Study of Pellet-Based Extrusion Deposition of Short, Long, and Continuous Carbon Fiber-Reinforced Polymer Composites for Large-Scale Additive Manufacturing. *J. Manuf. Sci. Eng.* **143**(7), (2021). <https://doi.org/10.1115/1.4049646>
101. Quan, Z., Larimore, Z., Wu, A., et al.: Microstructural design and additive manufacturing and characterization of 3D orthogonal short carbon fiber/acrylonitrile-butadiene-styrene preform and composite. *Compos. Sci. Technol.* **126**, 139–148 (2016). <https://doi.org/10.1016/j.compscitech.2016.02.021>
102. Hu, Y., Ladani, R.B., Brandt, M., et al.: Carbon fibre damage during 3D printing of polymer matrix laminates using the FDM process. *Mater. Des.* **205**, 109679 (2021). <https://doi.org/10.1016/j.matdes.2021.109679>
103. Araya-Calvo, M., López-Gómez, I., Chamberlain-Simon, N., et al.: Evaluation of compressive and flexural properties of continuous fiber fabrication additive manufacturing technology. *Addit. Manuf.* **22**, 157–64 (2018). <https://doi.org/10.1016/j.addma.2018.05.007>
104. Li, H., Wang, T., Joshi, S., et al.: The quantitative analysis of tensile strength of additively manufactured continuous carbon fiber reinforced polylactic acid (PLA). *Rapid Prototyping Journal* **25**(10), 1624–1636 (2019). <https://doi.org/10.1108/rpj-01-2018-0005>
105. Isobe, T., Tanaka, T., Nomura, T., et al.: Comparison of strength of 3D printing objects using short fiber and continuous long fiber. *IOP Conference Series: Materials Science and Engineering* **406**, 012042 (2018). <https://doi.org/10.1088/1757-899x/406/1/012042>
106. Wang, S., Li, Y., Xiang, H., et al.: Low cost carbon fibers from bio-renewable Lignin/Poly(lactic acid) (PLA) blends. *Compos. Sci. Technol.* **119**, 20–25 (2015). <https://doi.org/10.1016/j.compscitech.2015.09.021>
107. Tümer, E.H., Erbil, H.Y.: Extrusion-Based 3D Printing Applications of PLA Composites: A Review. *Coatings* **11**(4), 390 (2021). <https://doi.org/10.3390/coatings111040390>
108. Restrepo, I., Medina, C., Meruane, V., et al.: The effect of molecular weight and hydrolysis degree of poly(vinyl alcohol)(PVA) on the thermal and mechanical properties of poly(lactic acid)/PVA blends. *Polímeros* **28**(2), 169–177 (2018). <https://doi.org/10.1590/0104-1428.03117>
109. Lebedev, S.M., Gefle, O.S., Amitov, E.T., et al.: Mechanical properties of PLA-based composites for fused deposition modeling technology. *The International Journal of Advanced Manufacturing Technology* **97**(1–4), 511–518 (2018). <https://doi.org/10.1007/s00170-018-1953-6>
110. Benedetti, L., Brulé, B., Decreamer, N., et al.: Shrinkage behaviour of semi-crystalline polymers in laser sintering: PEKK and PA12. *Mater. Des.* **181**, 107906 (2019). <https://doi.org/10.1016/j.matdes.2019.107906>
111. Yang, C., Tian, X., Li, D., et al.: Influence of thermal processing conditions in 3D printing on the crystallinity and mechanical properties of PEEK material. *J. Mater. Process. Technol.* **248**, 1–7 (2017). <https://doi.org/10.1016/j.jmatprotec.2017.04.027>
112. Nawafleh, N., Celik, E.: Additive manufacturing of short fiber reinforced thermoset composites with unprecedented mechanical performance. *Addit. Manuf.* **33**, 101109 (2020). <https://doi.org/10.1016/j.addma.2020.101109>
113. Borowski, A., Vogel, C., Behnisch, T., et al.: Additive Manufacturing-Based In Situ Consolidation of Continuous Carbon Fibre-Reinforced Polycarbonate. *Materials (Basel)* **14**(9), 2450 (2021). <https://doi.org/10.3390/ma14092450>
114. Alarifi, I.M.: Mechanical properties and numerical simulation of FDM 3D printed PETG/carbon composite unit structures. *J. Market. Res.* **23**, 656–669 (2023). <https://doi.org/10.1016/j.jmrt.2023.01.043>
115. Shanmugam, V., Das, O., Babu, K., et al.: Fatigue behaviour of FDM-3D printed polymers, polymeric composites and architected cellular materials. *Int. J. Fatigue* **143**, 106007 (2021). <https://doi.org/10.1016/j.ijfatigue.2020.106007>
116. Li, S., Wang, K., Zhu, W., et al.: Contributions of interfaces on the mechanical behavior of 3D printed continuous fiber reinforced composites. *Constr. Build. Mater.* **340**, 127842 (2022). <https://doi.org/10.1016/j.conbuildmat.2022.127842>
117. Ekoi, E.J., Dickson, A.N., Dowling, D.P.: Investigating the fatigue and mechanical behaviour of 3D printed woven and nonwoven continuous carbon fibre reinforced polymer (CFRP) composites. *Compos. B Eng.* **212**, 108704 (2021). <https://doi.org/10.1016/j.compositesb.2021.108704>

118. Mohammadzadeh, M., Imeri, A., Fidan, I., et al.: 3D printed fiber reinforced polymer composites - Structural analysis. *Compos. B Eng.* **175**, 107112 (2019). <https://doi.org/10.1016/j.compositesb.2019.107112>
119. Flodberg, G., Pettersson, H., Yang, L.: Pore analysis and mechanical performance of selective laser sintered objects. *Addit. Manuf.* **24**, 307–315 (2018). <https://doi.org/10.1016/j.addma.2018.10.001>
120. Bernasconi, A., Cosmi, F., Dreossi, D.: Local anisotropy analysis of injection moulded fibre reinforced polymer composites. *Compos. Sci. Technol.* **68**(12), 2574–2581 (2008). <https://doi.org/10.1016/j.compscitech.2008.05.022>
121. Khudiakova, A., Berer, M., Niedermair, S., et al.: Systematic analysis of the mechanical anisotropy of fibre-reinforced polymer specimens produced by laser sintering. *Addit. Manuf.* **36**, 101671 (2020). <https://doi.org/10.1016/j.addma.2020.101671>
122. Jansson, A., Pejryd, L.: Characterisation of carbon fibre-reinforced polyamide manufactured by selective laser sintering. *Addit. Manuf.* **9**, 7–13 (2016). <https://doi.org/10.1016/j.addma.2015.12.003>
123. Chen, H., Zhu, W., Tang, H., et al.: Oriented structure of short fiber reinforced polymer composites processed by selective laser sintering: The role of powder-spreading process. *Int. J. Mach. Tools Manuf.* **163**, 103703 (2021). <https://doi.org/10.1016/j.ijmactools.2021.103703>
124. Dizon, J.R.C., Espera, A.H., Chen, Q., et al.: Mechanical characterization of 3D-printed polymers. *Addit. Manuf.* **20**, 44–67 (2018). <https://doi.org/10.1016/j.addma.2017.12.002>
125. Saroia, J., Wang, Y., Wei, Q., et al.: A review on 3D printed matrix polymer composites: its potential and future challenges. *Int. J. Adv. Manuf. Technol.* **106**(5–6), 1695–1721 (2019). <https://doi.org/10.1007/s00170-019-04534-z>
126. Czelusniak, T., Amorim, F.L.: Influence of energy density on selective laser sintering of carbon fiber-reinforced PA12. *Int. J. Adv. Manufact. Technol.* **111**(7–8), 2361–2376 (2020). <https://doi.org/10.1007/s00170-020-06261-2>
127. Lupone, F., Padovano, E., Pietroluongo, M., et al.: Optimization of selective laser sintering process conditions using stable sintering region approach. *Express Polym Lett* **15**(2), 177–192 (2021). <https://doi.org/10.3144/expresspolymlett.2021.16>
128. Okolie, O., Stachurek, I., Kandasubramanian, B., et al.: 3D Printing for Hip Implant Applications: A Review. *Polymers (Basel)* **12**(11), 2682 (2020). <https://doi.org/10.3390/polym12112682>
129. Takayanagi, A., Siddiqi, I., Ghanchi, H., et al.: Radiolucent Carbon Fiber-Reinforced Implants for Treatment of Spinal Tumors-Clinical, Radiographic, and Dosimetric Considerations. *World Neurosurg* **152**, 61–70 (2021). <https://doi.org/10.1016/j.wneu.2021.05.100>
130. Delaney, F.T., Denton, H., Dodds, M., et al.: Multimodal imaging of composite carbon fiber-based implants for orthopedic spinal fixation. *Skeletal Radiol.* **50**(5), 1039–1045 (2021). <https://doi.org/10.1007/s00256-020-03622-6>
131. Alia, M.H., Smagulova, Z., Otepbergenov, T.: Finite element analysis of the CFRP-based 3D printed ankle-foot orthosis. *Procedia Comput. Sci.* **179**, 55–62. (2021). <https://doi.org/10.1016/j.procs.2020.12.008>
132. Marinopoulos, T., Li, S., Silberschmidt, V.V.: Structural integrity of 3D-printed prosthetic sockets: Experimental study for paediatric applications. *J. Market. Res.* **24**, 2734–2742 (2023). <https://doi.org/10.1016/j.jmrt.2023.03.192>
133. Oladapo, B.I., Zahedi, S.A., Ismail, S.O., et al.: 3D printing of PEEK and its composite to increase biointerfaces as a biomedical material- A review. *Colloids Surf. B Biointerfaces* **203**, 111726 (2021). <https://doi.org/10.1016/j.colsurfb.2021.111726>
134. Han, X., Yang, D., Yang, C., et al.: Carbon Fiber Reinforced PEEK Composites Based on 3D-Printing Technology for Orthopedic and Dental Applications. *J. Clin. Med.* **8**(2), 240 (2019). <https://doi.org/10.3390/jcm8020240>
135. Davoodi, E., Fayazfar, H., Liravi, F., et al.: Drop-on-demand high-speed 3D printing of flexible milled carbon fiber/silicone composite sensors for wearable biomonitoring devices. *Addit. Manuf.* **32**, 101016 (2020). <https://doi.org/10.1016/j.addma.2019.101016>
136. Goh, G.D., Agarwala, S., Goh, G.L., et al.: Additive manufacturing in unmanned aerial vehicles (UAVs): Challenges and potential. *Aerosp. Sci. Technol.* **63**, 140–151 (2017). <https://doi.org/10.1016/j.ast.2016.12.019>
137. Azarov, A.V., Antonov, F.K., Golubev, M.V., et al.: Composite 3D printing for the small size unmanned aerial vehicle structure. *Compos. B Eng.* **169**, 157–163 (2019). <https://doi.org/10.1016/j.compositesb.2019.03.073>

138. Saputro, I.E., Wikarta, A., Muhtar, A.: Topology optimization on geometry of 3D printed “Impulse RC Alien 4 Inch” racing quadcopter frame with polylactic acid material. *AIP Conf. Proc.* **2187**, 050012 (2019). <https://doi.org/10.1063/1.5138342>
139. Siddique, S.H., Hazell, P.J., Wang, H., et al.: Lessons from nature: 3D printed bio-inspired porous structures for impact energy absorption – A review. *Addit. Manuf.* **58**, 103051 (2022). <https://doi.org/10.1016/j.addma.2022.103051>
140. Irfan, M.S., Patel, S., Umer, R., et al.: Thermal and morphological analysis of various 3D printed composite honeycomb cores. *Compos. Struct.* **290**, (2022). <https://doi.org/10.1016/j.compstruct.2022.115517>
141. Acanfora, V., Sellitto, A., Russo, A., et al.: Experimental investigation on 3D printed lightweight sandwich structures for energy absorption aerospace applications. *Aerosp. Sci. Technol.* **137**, (2023). <https://doi.org/10.1016/j.ast.2023.108276>
142. Dou, H., Ye, W., Zhang, D., et al.: Comparative study on in-plane compression properties of 3D printed continuous carbon fiber reinforced composite honeycomb and aluminum alloy honeycomb. *Thin-Walled Struct.* **176**, (2022). <https://doi.org/10.1016/j.tws.2022.109335>
143. Shibuya, Y., Zhang, J., Sato, Y., et al.: Enhancement of mechanical property and formability of CFRP core sandwich sheets by additive manufacturing process-induced material and structural anisotropies. *J. Mater. Process. Technol.* **310**, (2022). <https://doi.org/10.1016/j.jmatprotec.2022.117778>
144. Zhao, T., Yang, J., Chen, J., et al.: Review of carbon fiber-reinforced sandwich structures. *Polym. Polym. Compos.* **30**, (2022). <https://doi.org/10.1177/09673911221098729>
145. Fallah, A., Asif, S., Gokcer, G., et al.: 4D printing of continuous fiber-reinforced electroactive smart composites by coaxial additive manufacturing. *Compos. Struct.* **316**, (2023). <https://doi.org/10.1016/j.compstruct.2023.117034>
146. Zeng, C., Liu, L., Bian, W., et al.: 4D printed electro-induced continuous carbon fiber reinforced shape memory polymer composites with excellent bending resistance. *Composites Part B: Engineering* **194**, (2020). <https://doi.org/10.1016/j.compositesb.2020.108034>
147. Dong, K., Wang, Y., Wang, Z., et al.: Reusability and energy absorption behavior of 4D printed continuous fiber-reinforced auxetic composite structures. *Composites Part A: Appl. Sci. Manuf.* **169**, (2023). <https://doi.org/10.1016/j.compositesa.2023.107529>
148. Kang, Y., Wu, I., Tian, X., et al.: 4D printed thermally tunable metasurface with continuous carbon fibre. *Virtual Phys. Prototyp.* **18**(1), (2023). <https://doi.org/10.1080/17452759.2023.2224298>
149. Yan, W., Tian, X., Zhang, D., et al.: 3D Printing of Stretchable Strain Sensor Based on Continuous Fiber Reinforced Auxetic Structure. *Chin. J. Mech. Eng.: Add. Manuf. Front.* **2**(2), (2023). <https://doi.org/10.1016/j.cjmeam.2023.100073>
150. Wang, Z., Huang, Y., Zhang, X., et al.: Broadband underwater sound absorbing structure with gradient cavity shaped polyurethane composite array supported by carbon fiber honeycomb. *J. Sound Vib.* **479**, (2020). <https://doi.org/10.1016/j.jsv.2020.115375>
151. Yamamoto, K., Luces, J.V.S., Shirasu, K., et al.: A novel single-stroke path planning algorithm for 3D printers using continuous carbon fiber reinforced thermoplastics. *Addit. Manuf.* **55**, 102816 (2022). <https://doi.org/10.1016/j.addma.2022.102816>
152. Zhang, Q., Yang, X., Li, P., et al.: Bioinspired engineering of honeycomb structure – Using nature to inspire human innovation. *Prog. Mater. Sci.* **74**, 332–400 (2015). <https://doi.org/10.1016/j.pmatsci.2015.05.001>
153. Kuschmitz, S., Schirp, A., Busse, J., et al.: Development and Processing of Continuous Flax and Carbon Fiber-Reinforced Thermoplastic Composites by a Modified Material Extrusion Process. *Materials (Basel)* **14**(9), 2332 (2021). <https://doi.org/10.3390/ma14092332>

**Publisher’s Note** Springer Nature remains neutral with regard to jurisdictional claims in published maps and institutional affiliations.

Springer Nature or its licensor (e.g. a society or other partner) holds exclusive rights to this article under a publishing agreement with the author(s) or other rightsholder(s); author self-archiving of the accepted manuscript version of this article is solely governed by the terms of such publishing agreement and applicable law.